To the Graduate Council:

I am submitting herewith a thesis written by Sudha Sunil Chhaya entitled "Role of Iron and Aluminum in Brain Metabolism." I have examined the final copy of this thesis for form and content and recommend that it be accepted in partial fulfillment of the requirements for the degree of Master of Science, with a major in Biochemistry.

J. G. Joshi, Major Professor

We have read this thesis
and recommend its acceptance:

Walter Farkas

Engin Serpersu

Accepted for the Council:

Vice Provost and
Dean of the Graduate School

ROLE OF IRON AND ALUMINUM
IN
BRAIN METABOLISM

A thesis presented for the

Master of Science

Degree

The University of Tennessee, Knoxville

SUDHA SUNIL CHHAYA

May, 1995

DEDICATION

To my dearest sister, Vani

and

To my loving husband, Sunil.

ACKNOWLEDGEMENTS

I would like to thank Dr. Jayant G. Joshi for his guidance, my committee members Dr. Walter Farkas and Dr. Engin Serpersu for their valuable time and suggestions. Thanks are due to Dr. Vijay Chauthaiwale and to Dr. Madhu Dhar for their constant help and encouragement throughout my laboratory work. I would like to thank immensely, Dr. John Koontz for his kind understanding and patient help during various stages of my graduate study. Dr. Sivadasan and the students of Dr. Rouse's lab have helped me immensely in experimentation and trouble-shooting. I would like to thank my parents for their love and support. I would like to thank *most*, my dear husband for his unflinching help and remarkable wit all along.

TABLE OF CONTENTS

LIST OF FIGURES

LIST OF TABLES

ABSTRACT

Ferritin is a storage protein for excess iron. It is composed of heavy (H) and light (L) chain subunits. In brain and other tissues, the ferritin heavy chain (FTH) is coded by two mRNAs of 1.1kb and 1.4kb. The 1.4kb mRNA has an additional 279nt in the 3'UTR (untranslated region) upstream to the polyA$^+$ tail. In all other respects, the two mRNAs are identical. The 1.4kb FTH mRNA is most abundant in the brain compared to other tissues such as liver, heart, pancreas, intestine, skeletal muscle, kidney and placenta. Earlier studies have found that of the two FTH mRNAs, the 1.1kb is more abundant than the 1.4kb mRNA in the human liver. It is shown in this study that even in the human brain, the 1.1 kb mRNA is more abundant than the 1.4kb mRNA.

Human fetal brain shows the presence of a non-ferritin mRNA (1.55kb) containing a part of, or the entire 279nt which is present in the 3'UTR of the 1.4kb FTH mRNA. No similar mRNA is detected in the human adult brain. Changes in the genome during the life span of humans as with any organism are unlikely. The above observation, therefore, suggests the occurrence of development-dependent changes in human brain cells that result in the transcriptional switching-off of a certain yet unidentified gene between fetal and adult stages of life.

Aluminum (Al^{3+}) is a metal ion that has no physiological function. But as it resembles iron (Fe) in its co-ordination chemistry, it is

suggested that Al^{3+} uses the transport mechanism of iron *in-vivo*. Earlier researchers have isolated Al^{3+}-transferrin and Al^{3+}-ferritin complexes from human serum and the brains of aluminum fed rats. Al^{3+} has been shown to inhibit several regulatory enzymes of cellular metabolism. We show in this study the effect of the metal ion on two regulatory enzymes, namely aconitase and isocitrate dehydrogenase (ICDH). Cytosolic aconitase is a regulating protein of ferritin biosynthesis and is not affected by Al^{3+} while ICDH, a key regulatory enzyme and control point of the TCA cycle, is inhibited by the metal ion in a concentration-dependent manner. Al^{3+} exhibits a competitive inhibition with respect to $NADP^{+}$ (a substrate for ICDH) with a K_i of $7.41 \times 10^{-4}M$.

A similar inhibition *in-vivo* of ICDH, may deregulate the TCA cycle, affecting not only the complete oxidation of glucose, but also the synthesis of amino acids and porphyrins.

PART I

INTRODUCTION

Iron is a metal ion of great physiological significance due to its role in biocatalysis and oxygen transport. It exists predominantly in two oxidation states, as Fe^{2+} and Fe^{3+}. At physiological pH, Fe^{3+} is insoluble and non-toxic, whereas Fe^{2+} is soluble and toxic (1). In living systems, excess iron is stored and released on demand by the storage protein, ferritin. Each ferritin molecule is comprised of a total of 24 subunits of heavy (H, Mr 22,000) and light (L, Mr 19,000) chains. Ferritin heavy chain (FTH) is more acidic and has a ferroxidase center that oxidizes Fe^{2+} to Fe^{3+}. The reduced iron is then stored as ferrichydroxyphosphate by the L chains in the core of the ferritin protein.

The subunits of ferritin form a protein shell which can store in its central cavity up to a maximum of 4500 g atoms of iron, bound as ferric-hydroxyphosphate (2). When required, the bound iron is reduced to Fe^{2+} and released to a chelator that binds and transports it to the site where it is required. Though the exact mechanism of reduction *in-vivo* is yet unclear, it is known to require a reductant (such as ascorbic acid) and an iron chelator (such as ferritin) *in-vitro* (1).

Besides storing and transporting iron, ferritin functions as a metal ion detoxicant. It binds Cu^{2+}, Zn^{2+}, Cd^{2+}, Be^{2+}, Pb^{2+} and Al^{3+} *in-vitro* and *in-vivo* (4,5,6,7). Ferritin *in-vitro* protects against and

reverses the inhibition by beryllium (Be^{2+}) of the enzymes $Na^{+}K^{+}$ATPase, alkaline phosphatase, RNA polymerase and phosphoglucomutase (3). Studies have shown that the administration of iron salts to rats elevated their ferritin synthesis and helped them survive otherwise toxic doses of Be^{2+} (8). Since ferritin functions both as a metal chelator and metal donor, its capacity to bind non-ferrous metal ions may be crucial in metal ion transport and metabolism in living systems. Ferritin may be one of the factors governing the production of energy in the cell (9). The protein has also been suggested to play an important role in the regulation of myelopoiesis (1).

Ferritin preparations from the human brain separate into two bands by SDS-PAGE. These bands correspond to the H and L chain subunits (11). Ferritins differing in the composition of H and L chains are called isoferritins. In the human brain and other tissues, each protomer of ferritin consists of a total of 24 subunits of H and L chains; theoretically, therefore, 25 different isoferritins are possible that vary in the proportion of H and L chains. Upon isoelectric focusing (IEF), native ferritin isolated from a single source separates into several bands which are isoferritins varying in net charge. Isoferritins are present in various proportions of the two chains in different tissues; their ratio depends on the iron state of the cell. H- chain rich acidic isoferritins have been found

to sequester less iron than L- chain rich basic isoferritins (12). As isoferritins differ in their capacity to store iron, they may have corresponding differences in their capacities to bind and release other metal ions as well. The isoferritin profile of one tissue may well be different from another.

The brain is metabolically one of the most active organs in the body. It is the center of unceasing electrical activity, providing excitation and stimulation through the nervous tissue throughout the body. Iron is found in appreciable quantities in the brain tissue with significant variations in concentration in different areas and a correspondingly unique isoferritin profile. Drastic changes in the brain biochemistry and impaired functioning may occur in iron deficiency (13).

Close to 30% of the total non-heme iron in the brain is stored as ferritin (14). The rest is thought to be an important participant in the metabolism of neurotransmitters. Human liver ferritin on isoelectric focusing (IEF) gives 5 major and 4 minor acidic bands between the pI's of 4 - 5.5 (15). But human brain ferritin (HBF) resolves into around 20 bands, with a wider pI range, only 5 of which overlap with liver ferritin. This suggests that the brain contains a greater number of isoferritins than those in the liver and probably other tissues.

The brain is a highly aerobic tissue. It therefore requires a high level of oxygen. It also contains large concentrations of ascorbate, a physiological reductant (1). The presence of a reductant such as ascorbate, an iron chelator such as ferritin and oxygen creates an environment conducive not only for the favorable process of iron reduction but also for the unfavorable and harmful process of generation of free radicals. Fe^{2+}, in the presence of dioxygen (O_2) gets oxidized, thereby reducing oxygen to form O_2^-, a free radical (16). O_2^- being highly reactive attacks cellular components most importantly lipids, such as polyunsaturated fatty acids of phospholipids, causing irreparable membrane damage (17). It is therefore extremely important that iron binding and release is highly regulated, particularly in the brain tissue so as to avoid free radical induced lipid peroxidation. Iron metabolism may be regulated in a much more critical manner in this organ than in other tissues, perhaps due to the greater number of isoferritins, their specificity and distribution in the brain.

High pressure liquid chromatography (HPLC) resolved HBF-holoferritin into two clusters of peaks. The first cluster of 7 (with 2 major and 5 minor) peaks could be identified as H chain components as they migrated with an R_f value similar to that of the H chain of human brain ferritin on an SDS-polyacrylamide gel electrophoresis. Also, subunits prepared from HBF (apoferritin), as

a control for possible free radical damage during isolation of holoferritin subunits, gave an identical HPLC profile. Both of these HPLC results were reproducible. The presence of more than 1 peak on HPLC indicated that the H chain subunit was heterogeneous (18).

Experiments were done to further investigate the heterogeneity of the ferritin heavy chain (FTH). The HPLC fractions of H chain were analyzed for amino acid composition by the acid hydrolysis procedure. All the H chain fractions were found to be essentially identical in amino acid composition (18). Analysis of the amino acid composition by acid hydrolysis has some difficulties. During the procedure, glutamine and asparagine get converted to glutamic acid and aspartic acid respectively. Therefore, the difference between the -amine and the -acid cannot be identified by the acid hydrolysis procedure. Besides, tryptophan and methionine rapidly get destroyed during the procedure and their contribution to the amino acid composition cannot be determined. As determining the amino acid composition by acid hydrolysis of the human brain ferritin H chain subunit did not explain its heterogeneity on HPLC, experiments were done to sequence the gene coding the H chain of human brain ferritin.

The coding sequence of the 1.1kb FTH mRNA in the human adult

brain and liver are identical. Two normal adult brain cDNA libraries were therefore screened using a human liver FTH cDNA as a probe. Six positive recombinants were obtained. Their cDNA's were subcloned into a plasmid vector, pBluescript (pBSK)(+) by *in-vivo* excision and directed cloning. Agarose gel analysis and sequencing of the restriction digested cDNA inserts showed that their insert sizes ranged from 0.5 to > 1.0kb. Five of the recombinants upon complete sequencing showed that they were identical to the liver FTH cDNA except for the presence of two cytosines inserted at the 16 and 40 positions of the 3' UTR. Yet, none of the inserts were full length indicating that the human adult brain cDNA library may have been incomplete (19).

In order to obtain a full length clone for FTH, a cDNA library from an 11- week old human fetal brain was screened using the human liver ferritin H chain (FTH) encoding cDNA as probe. Four positive recombinants pcFB1, pcFB2, pcFB3 and pcFB4 were obtained. Their cDNA's were subcloned into the vector pBSK(-), and transformed into *E. coli* (XL1 blue) cells. Sequence analysis of the inserts from the transformed bacteria of pcFB2-4 showed that they were identical to the published sequence of human liver FTH cDNA (20). They contained the 158bp of the 3' UTR, the entire coding region of 549bp (183 amino acids) and the 215bp of the 5' UTR. The sequence of cFB1 showed that it contained an additional sequence

of 279bp upstream to the polyA$^+$ tract. While cFB2-4 had only one polyadenylation signal, cFB1 showed the presence of two 5' AAUAAA sequences (polyadenylation signals) at the 16bp and at 296bp upstream to the polyA$^+$ tract. The second signal has been known to be used in the processing of the liver FTH pre-mRNA. cFB1, therefore, may have been copied from an RNA that was processed at an alternate polyA$^+$ site to generate a mature FTH mRNA (20).

The above studies clearly showed that in addition to the published liver FTH mRNA (1.1kb), there is a second FTH mRNA (1.4kb) in the brain that contains a novel sequence of 279nt at its 3' end. In all other respects, its sequence is identical to the published sequence of liver FTH mRNA. Northern blot analysis showed the presence of the novel FTH mRNA in other human tissues. Its relative concentration was highest in the brain compared to other organs, such as, the kidney, lung, skeletal muscle, pancreas, heart, placenta and the liver. Of the two, the 1.1kb FTH mRNA was found to be more abundant than the 1.4kb mRNA in the liver (19). The aim of this study was to investigate the percent contribution of the 1.4kb transcript to the cumulative FTH mRNA in the human brain.

Northern blot analysis of fetal brain polyA$^+$ RNA using the cDNA of 279nt of the 3' UTR of the 1.4kb FTH mRNA showed two hybridizing bands of 1.55 and 1.4kb. Further analysis using the FTH structural gene as probe showed that while the 1.4kb band was due to the ferritin H-chain mRNA, the 1.55kb band was due to a non-ferritin, mRNA as yet unidentified (21). The present study was aimed also at investigating the presence of a similar 279nt containing non-ferritin mRNA in the human adult brain.

To date, the role of the novel sequence of 279nt in stability or translation of the longer transcript and its overall significance in the FTH synthesis is unknown. The fundamental reason for the presence of seven peaks of HBF H chain, though their amino acid composition is similar, is also unknown.

The synthesis and regulation of H and L chains of ferritin are iron dependent. When intracellular levels of iron are low, translation of the H- and L- chain m-RNA is repressed and when the iron levels within the cell increase due to absorption, translation is derepressed causing a 100-fold increase in the rate of ferritin synthesis (22). This regulation is achieved due to the presence of a 28nt stem-loop structure called the iron responsive element (IRE) in the 5'UTR of the FTH m-RNA of ferritin H-chain mRNA's. The IRE is specifically recognized and bound by a protein called the

IRE-binding protein (IRE-BP) (23) alternately referred to as IRF (24).

As an important enzyme of the tricarboxylic acid (TCA) cycle, aconitase is present in the mitochondria (m-aconitase), the site of the TCA cycle. Studies have revealed the presence of a second aconitase found exclusively in the cytosol of mammalian tissues. It is called the cytosolic aconitase (c-aconitase). The c-aconitase is distinct from the m-aconitase (25). All active site residues are conserved in both m- and c-aconitase, both have a Fe-S cluster that they require in the 4Fe-4S form for enzymatic activity and both catalyze the conversion of citrate to aconitate and isocitrate in different compartments of the cells. c-Aconitase and m-aconitase have similar turnover number, affinities and activities with all the three substrates namely, citrate, *cis*-aconitate and isocitrate as measured in units/nmol of the cluster; yet, the two enzymes show a number of differences. Upon isoelectric focusing of the three forms of both c-aconitase and m-aconitase, the pI values of the [3Fe-4S] and [4Fe-4S] forms of c-aconitase were found to be close to 8.0 whereas those of the same forms of m-aconitase were between 7.5 and 7.8. The apoprotein formed by oxidative removal of the cluster by ferricyanide showed that the pI of apo c-aconitase decreased to approximately 7.7 while that of apo m-aconitase increased to approximately 8.0. The m-aconitase

was isolated as containing the iron-sulfur cluster in the [3Fe-4S] form and needed activation by the addition of external iron whereas c-aconitase was isolated as active enzyme, apparently with a [4Fe-4S] cluster. Amino acid analysis of c-aconitase revealed that it had 30% homology with the mitochondrial enzyme. The EPR spectrum of c-aconitase was also different from that of m-aconitase (25).

When isolated from cells depleted in iron, c-aconitase bound the 28nt stem loop structure, the IRE of mRNA's and was inactive as an enzyme. Upon external addition of iron, or when isolated from cells grown in iron rich media, c-aconitase showed high enzymatic activity, but its RNA binding was abolished. The change in enzymatic activity manipulating levels of iron was reflected by a concomitant change in RNA binding by the protein. Interestingly, m-aconitase, did not show any RNA binding activity irrespective of iron manipulation.

Further characterization of c-aconitase revealed that it was strikingly similar to the published sequence of IRE-BP. Both proteins contained a single Fe-S cluster and both either bound RNA or were enzymatically active. Purified IRE-BP, upon iron-loading, exhibited a loss of RNA-binding with a rise in aconitase activity. Iron manipulation reciprocally affected aconitase activity

and RNA binding of IRE-BP both *in-vitro* and *in-vivo*. Comparison of the sequence of aconitase purified from cytoplasmic extracts showed that it is identical to the IRE-BP in amino acid composition, molecular weight, isoelectric point and the sequences of six random peptides (25). This led to the conclusion that c-aconitase is IRE-BP and the same protein alternates between the enzymatic and repressor roles by virtue of its iron-sulfur cluster (25). A fully filled Fe-S (4Fe-4S) cluster is required for aconitase activity, but RNA binding requires no specific status of the cluster. In fact, it is not yet clear if the cluster in the active repressor form of the protein has 1Fe-4S, 2Fe-4S or 3Fe-4S cluster. Aconitase activity in cytoplasmic extracts is therefore, a reciprocal measure of RNA-binding and a direct measure of ferritin synthesis.

The role of the iron-sulfur (Fe-S) cluster in the dual function of IRE-BP is interesting. The Fe-S cluster probably acts as a metal switch *in-vivo* that enables the protein to function either as a translational repressor or as an active enzyme. Haile *et al* have proposed that a single protein could exist in either of the two conformations: "open" that has a high affinity RNA-binding but no aconitase activity, and "closed" that is active as an aconitase but does not bind RNA (53). These conformations could be determined by the number of iron atoms in the Fe-S cluster which in turn depends on the iron status of the cell. The "closed" conformation of

the protein may be favored by the 4Fe-4S cluster that results due to high intracellular iron. It is speculated that crucial interactions exist between the domains of the protein, the Fe-S cluster and the substrate, which may be weakened in the absence of the substrate and a partially filled Fe-S cluster, resulting in the "open" conformation. In this conformation, the RNA-binding site of the protein could be exposed, that probably includes the aconitase active site cleft (53).

Aluminum (Al^{3+}) accounts for 8% of the earth's crust and is present in combined form in minerals. The ocean concentration of Al is below 1µg/l since diatoms accumulate Al and silicon (26). Fresh water reservoirs contain very little Al^{3+}. Unfortunately, widespread industrialization and resulting acid precipitation, has caused a steady and rapid decrease in the pH of lakes and other natural fresh water sources. Continued acidification causes leaching of Al from soil and sediments. This creates an environment favoring increased solubility of the metal ion in water, making it available to biological systems at concentrations in which it is toxic (27). As a food and water contaminant, the daily intake of Al in humans is estimated to be around 20 mg/day via the gastrointestinal tract and about 3-15 µg/day by inhaling. The plasma level of Al is approximately 7µg/l (27).

At neutral pH, Al precipitates in solution as $Al(OH)_3$ that redissolves to form tetrahedral aluminate, $Al(OH)_4^-$ which is the primary Al(III) species at pH > 6.2. But, as the solution becomes more acidic, successive deprotonation occurs to form soluble $Al(OH)_3$, $Al(OH)_2^+$ and $Al(OH)_4^-$. At pH below 5.0, Al(III) exists predominantly as the highly soluble octahedralhexahydrate $Al(H_2O)_6^{3+}$. In biological systems, in the presence of ligands, a high total Al(III) occurs as a polynuclear species, the composition of which is time-dependent (26).

Al^{3+} resembles Fe^{2+} in its co-ordination chemistry, the ionic radius and hydrolysis behavior. Therefore, it has been suggested that Al^{3+} may use the same transport and storage mechanisms as Fe^{3+} *in-vivo* (28). Strong evidence for this comes from *in-vitro* studies showing the interaction of Al^{3+} with physiological ligands such as transferrin (29), ferritin (30), citrate and phosphate (31) and *in-vivo* studies resulting in the isolation of Al^{3+}-transferrin and Al^{3+}-ferritin complexes from human serum and the brains of rats that have been fed with low levels of $AlCl_3$ (100μM) (29,15).

The livers of Al^{3+}-fed rats contain very little Al^{3+} as compared to their brains. This suggests that Al^{3+} may be cleared from the liver and other tissues and is accumulated in the brain where it is chelated by ferritin so as to avoid the inhibition of enzymes (32).

There is a very low Al^{3+} flux into cells and across the blood brain barrier. This may be the reason why, short-lived cells are not able to accumulate Al^{3+} but long lived cells such as neurons in the brain accumulate toxic levels of the metal ion (27).

The physiological effects of Al^{3+} are numerous and harmful. Al^{3+} and calcium (Ca^{2+}) accumulate in degenerated brain areas and neurofibrillary tangles (52). Neurochemical studies of brain tissue of deceased Alzheimer's disease (AD) patients have revealed that they contain elevated total Al^{3+} levels, suggesting that the metal ion plays a significant role in the development of the disease (34). In senile dementia, hippocampal neurons containing neurofibrillary tangles showed foci of high Al^{3+} concentration in the nuclear region, under electron microscopy and x-ray spectroscopy (35). Al^{3+} has been shown to play a pivotal role in the development of renal dialysis encephalopathy (36). Al has also been implicated in increasing the permeability of the erythrocyte membrane making lipids more accessible to iron. This may in turn accelerate the lipid peroxidation initiated by the free radicals made available by iron (10).

Al^{3+} increases the permeability of the blood-brain barrier that could contribute to neuronal disorders (37). When bound to protein, Al^{3+} causes it to be more randomly coiled than the native

protein (39). The protein calmodulin (CaM), when bound to Ca^{2+}, regulates several phosphorylation-dephosphorylation reactions. Al binds to CaM and disrupts its function (40). The activity of CaM is restored by the chelation of Al by a metal binding protein such as transferrin. The phosphate content of the iron core determines the amount of Al bound to the protein *in-vitro*. Studies with phosphate containing and phosphate free synthetic iron cores showed that the phosphate containing cores bound more non-ferrous metal ions than the phosphate-free cores(30).

Ferritin may bind Al^{3+} as it is a nonferrous metal ion detoxicant in living systems. When bound to ferritin in high concentrations, Al^{3+} interferes with the primary functions of the protein such as iron binding, storage and metal ion detoxication. The binding of a high concentration of Al^{3+} to human brain ferritin decreases the rate of iron uptake by the protein in a concentration dependent manner (43).

Specific isoferritins are selectively located in different regions of the tissue; isoferritins have also been suggested to have a vital role in cellular regulation. The effect of Al^{3+} binding may therefore have differential effects in some isoferritins as compared to others. Alteration of isoferritin function thereby upsets their normal cellular regulation. Al^{3+}-ferritin complexes

have been isolated from the brains of humans who died of AD (44). Since the available ferritin in the brain is used to chelate Al, the unchelated Fe^{2+} may cause increased ferritin synthesis.

Perhaps the most serious effects of Al^{3+} occur due to its interference with the regulatory steps of cellular metabolism. Numerous rate-limiting steps and their corresponding enzymes are inhibited by Al^{3+}. The following are examples of regulatory enzymes that are inhibited by Al^{3+}. The enzymes hexokinase and glucose-6-phosphate dehydrogenase (G6PDH) catalyze the rate-limiting steps of glycolysis and pentose phosphate pathway respectively. Both of these are inhibited by Al^{3+} (45, 46). Free Al^{3+} has been demonstrated to potently inhibit signal transduction mediated by the G protein from retinal rods photoreceptors (G_V) by exhibiting competition with Mg^{2+}, an essential cofactor for the nucleotide exchange catalysis of the G protein. The GDP/GTP nucleotide exchange is the first and rate-determining step in the amplification of signal from receptor to effector mediated by the G proteins (47). Although Al^{3+} can effectively substitute for Mg^{2+} at the molecular level, it is not competent in catalysis due to the charge difference in the cations. The substitution of Al^{3+} for Mg^{2+} in enzymes and consequent inhibition of catalysis is suggested to be the underlying mechanism for Al^{3+}- mediated toxicity (47).

In rat brain slices, the carbachol stimulated hydrolysis of phosphoinositides was inhibited by $AlCl_3$ in a dose-dependent manner (48). The rate limiting step in acetylcholine synthesis, which reflects the cholinergic activity *in vivo*, is high affinity choline transport. This transport was inhibited by Al^{3+} *in-vitro* (33). It has been shown earlier that acetylcholine esterase and calmodulin-dependent Ca^{2+}/Mg^{2+} ATPase, which are both regulatory enzymes, are inhibited by Al^{3+} (49, 50).

Na^{+}/ K^{+} ATPase, an enzyme that maintains the sodium electrochemical gradient across the cell membrane, is vital for the high affinity transport of GABA, glutamate, choline, dopamine, noradrenaline and serotonin. The transport of many of these neurotransmitters in synaptosomes governs nerve transmission. Al^{3+} inhibits the Na^{+}/K^{+} ATPase and the transport of the above neurotransmitters in a concentration dependent manner (51). Al^{3+} interferes with many regulatory enzymes such as adenylate cyclase, 3',5' cyclic nucleotide phosphodiesterase, alkaline phosphatase, catechol-O-methyl transferase and ferroxidase (42).

The tricarboxylic acid (TCA) cycle is an important pathway in living systems. The final product of glycolytic breakdown of glucose is pyruvate which undergoes oxidative decarboxylation to form acetyl coenzyme A. This activated acetyl unit is then

completely oxidized to CO_2 by the TCA cycle. The TCA cycle is not only a significant pathway for the generation of energy, but also the final common pathway connecting the metabolism of amino acids, fatty acids and carbohydrates (38).

The TCA cycle is regulated at three control points, namely, the synthesis of citrate, the formation of α - ketoglutarate (by the enzyme isocitrate dehydrogenase (ICDH)) and the formation of succinyl CoA. The enzyme ICDH is the second regulatory enzyme and the rate of its reaction controls the overall rate of the TCA cycle. ICDH is allosterically regulated by isocitrate, ADP, NADP, NAD and Mg^{2+}. The enzyme preceding it in the TCA cycle is aconitase. Aconitase catalyzes the conversion of citrate to *cis*-aconitate, which is subsequently converted to isocitrate. Both reactions are reversible. The equilibrium concentrations of citrate, aconitate and isocitrate are 90.9%, 2.9% and 6.2% respectively. The affinities of the porcine heart aconitase for citrate, aconitate and isocitrate are 3.6×10^{-3}M, 1.2×10^{-4}M and 4.8×10^{-4}M respectively. The enzyme thus has the highest affinity for isocitrate (41). By dehydrogenating and decarboxylating isocitrate, ICDH converts it into α-ketoglutarate. Thus, by the removal of isocitrate, a product of the reaction of aconitase, ICDH pulls the equilibrium of the aconitase reaction towards the utilization of citrate to form isocitrate. ICDH is thus important in regulating the

citrate levels within the cell. As elucidated earlier, c-aconitase (or IRE-BP) is an important regulatory protein of ferritin biosynthesis.

The experimental approach of this study addresses the following:

1. (a) The percent contribution of the 1.4kb FTH mRNA to the total FTH mRNA in the human adult brain.
   (b) Analysis of human adult brain polyA$^+$ RNA to investigate for the presence of 279nt containing nonferritin mRNA.
2. The effect of aluminum on the regulatory proteins, aconitase and isocitrate dehydrogenase.

REFERENCES

1. Joshi, J.G. and Clauberg, M. (1988) Biofactors, 1, 207 -212
2. Aisen, P. and Listowski, I. (1980) Ann. Rev. Biochem., 49, 357 -393
3. Price, D.J. and Joshi, J.G., (1984) Toxicology, 31, 151 - 163
4. Wardeska, J.G., Violione, B. and Chasteen, N.D. (1986) J. Biol. Chem., 261, 6677 - 6683
5. Price, D.J. and Joshi, J.G. (1982) Proc. Natl. Acad. Sci. USA., 79, 3116-3119
6. Price, D.J. and Joshi,J.G. (1983) J. Biol. Chem., 258, 10873 -10880
7. Lindenschmidt, R.C., Sendelbach, L.E., Witschi, H.P., Price, D.J., Fleming, J.T. and Joshi, J.G. (1986) Toxicol. Appl. Pharmacol., 82, 344 - 350
8. Joshi, J.G., Sczekan, S. and Fleming, J.T. (1989) Biol. Trace Elements Res., Vol 21, 105 - 110
9. Thiel, E.C. (1983) in Thiel, E.C., Eichorn, G.L. and Marzilli, L.G. (eds), "Advances in Inorganic Biochemistry", Elsevier, New York, vol 5, 1 - 38
10. Spiro, T.G., Pape, L. and Saltman, P. (1967) J. Am. Chem. Soc., 89, 5555 - 5562
11. Fleming, J.T. and Joshi, J.G. (1988) FASEB J., 2, PA 766, abstr. no. 2730
12. Konijn, A.M., Tal, R., Levy, R. and Matzner, Y., Anal. Biochem.,

144, 423 - 428

13. Skikne, B.S., Lynch, S.R., Oke, A.F. and Cook, J.D. (1987) in Eighth International Conference on Proteins of Iron Transport and storage May 10 -14 abstr. no. 119
14. Mulligan, M. and Linder, M. (1983) in "The Biochemistry and Physiology of Iron" (Saltman, P. and Hagenaver, J., eds), p313, Elsevier, New York
15. Fleming, J.T. and Joshi, J.G. (1987) Proc. Natl. Acad. Sci. USA., 84, 7866 - 7870
16. Fridovich, I. (1975) Ann. Rev. Biochem., 44, 147 - 159
17. Siesjo, B.K. (1978) in "Membrane damage due to free radicals" in "Brain energy metabolism", John Wiley & Sons, New York
18. Fleming, J. (1989) "Studies on brain ferritin", Ph.D thesis, University of Tennessee
19. Dhar, M.S. and Joshi, J.G. (1993) J. Neurochem., 61, 2140 - 2146
20. Dhar, M., Chauthaiwale, V. and Joshi, J.G., (1993) Gene, 126, 275 - 278
21. Dhar, M.S. and Joshi, J.G. (1994) Biofactors, Vol 4 no. 3/4, 147 - 149
22. Dhar, M., Chauthaiwale, V. and Joshi, J.G., (1993) Gene, 126, 275 - 278
23. Leibold, E.A. and Munro, H.N. (1988) Proc. Natl. Acad. Sci. USA., Vol 85, 2171 - 2175
24. Mullner. E.W., Neupert, B. and Kuhn, L.C., (1989), Cell, vol 58,

373 - 382

25. Kennedy,M.C., Mueller, M.L., Blondin, G.A. and Bienert, H. Proc. Natl. Acad. Sci., USA, vol 89, 11730- 11734
26. Martin, J.B. (1991) in "Aluminum in biological systems" in"Aluminum in chemistry, biology and medicine: A series of advances", Vol 1, Nicolini, M., Zatta, P.F. and Corain, B. (eds) Raven press, New York.
27. Havas, M. and Liken, G.E. (1985) Can. J. Zool., 63, 1114 - 1119
28. Crumbliss, A.L. and Garrison, J.M. (1988) Comments InOrg. Chem., 8, 1 - 26
29. Trapp, G.A. (1983) Life. Sci., 33, 311 - 316
30. Sczekan, S.R. and Joshi, J.G. (1989) Biochim. Biophys. Acta., 990, 8 - 14
31. Martin, J.B. (1986), J. Inorg. Biochem., 28, 181 - 187
32. Morris, C.M., Candy, J.M., Court, J.A., Whitford, C.A. and Edwardson, J.A. (1987) Biochem. Soc. Trans., 15, 498
33. Drachman, D. A., and Leavitt, J., (1974) Arch. Neurol., 30, 113 - 117
34. Crapper, D.R., Krishnan, S.S. and Dalton, A.J. (1973) Science, 180, 511 - 513
35. Perl, D.P. (1980) Science, 208, 297 - 299
36. Alfrey, A.C., LeGendre, G.R. and Kaehny, W.D. (1976) N. Engl. J. Med., 294, 184 - 188
37. Wisniewski, H.M. and Sturmann, J.A. (1989) In Gitelman,

H.J.(ed), "Neurotoxicity of Aluminum" in "Aluminum and Health", Marcel Dekkar, New York, 125 - 165

38. Stryer, L. (1981) in "Biochemistry", W.H. Freeman, and Company, San Fransisco, 288 - 290
39. Siegal, N. and Hang, A. (1983) Biochim. Biophys. Acta, 744, 36 - 45
40. Putteril, J.J. and Gardner, R.C. (1988) Biochim. Biophys. Acta, 964, 137 - 145
41. Barman, T. E., (1969) in "Enzyme Handbook", Springer - Verlag, New York, II, 766
42. Ganrot, P.O. (1986) Environ. Health. Perspect. 65, 363 - 441
43. Fleming, J.T. and Joshi, J.G. (1991) Neurobiol. Aging, 12, 413 - 418
44. King, S.W., Savory, J. and Wills, M.R. (1981) CRC Crit. Rev. Clin. Lab. Sci., 14, 1 - 20
45. Womack, F.C. and Colowick, S.P. (1979) Proc. Natl. Acad. Sci. USA., 76, 5080 - 5084
46. Cho, S.W. and Joshi, J.G. (1989) Biochemistry, 28, 3613 - 3618
47. Miller, J.L., Hubbard, C.M., Burlon, J.L. and MacDonald, T.L. (1989) J. Biol. Chem., 264, 243 - 250
48. Johnson, G.V.W. and Jope, R.S. (1986) Toxicology, 40, 93 - 102
49. Marquis, J. K., and Lerrick, A. J., (1982) Biochem. Pharmacol., 31, 1437
50. Garza, R., Equivel, C. and Ross, D. H., (1984) Soc. Neurosci.

Abstr., 10, 416

51. Lai, J. C. K., Leung, T. K. C., Lim, L. and Davidson, A. N., (1980) Biochem. Pharmacol., 29, 141

52. Yoshimasu, F., Uebayashi, Y., Yoshira, Y., Iwata, S. and Sasajima, K. (1976) Folia. Psych. Neuro. Jap., 30, 49 - 55

53. Haile, D.J., Rouault, T.A., Tang, C. K., Chin. J., Harford, J.B. and Klausner, R.D. (1992) Proc. Natl. Acad. Sci., USA., 89, 7536 - 7540

PART II

ESTIMATION OF THE PERCENT CONTRIBUTION OF THE 1.4kb mRNA TO THE TOTAL FERRITIN HEAVY CHAIN mRNA

Summary

Two mRNAs of length 1.4 and 1.1kb code for ferritin H chain. The 1.4kb mRNA contains an additional 279nt sequence at its 3'untranslated region. In all other respects the two mRNAs are identical. We show here that the 1.1kb mRNA is in greater abundance in the human liver and brain. Human fetal brain shows the presence of non ferritin mRNA of 1.55kb containing a part of, or the entire 279nt which is present in the 3' untranslated region (UTR) of the 1.4kb FTH mRNA. No similar mRNA could be detected in the human adult brain. This observation suggests that development-dependent changes may occur in the brain cells resulting in switching off of the transcription of certain genes between the fetus and adult stages of life.

Background

Ferritin is the ubiquitous storage protein for excess iron in living systems. Each molecule of ferritin is made up of a total of 24 subunits of heavy (H, Mr 22,000) and light (L, Mr 19,000) chains (1). Two mRNAs of length 1.4 and 1.1kb code for the ferritin H chain (FTH). These are identical in the 5' UTR, the coding region, the 3' UTR and a stem loop structure of 28nt within the 5' UTR called the iron responsive element (IRE) (2). Fig 2.1 is a diagrammatic representation of the two FTH transcripts. The 1.4kb FTH mRNA has an additional 279nt upstream to the polyA$^+$ tail (3). The role of this novel sequence in stability or translation of the 1.4kb mRNA and its overall significance in the FTH synthesis is yet unknown. The aim of this study was to investigate the percent contribution of the 1.4kb mRNA to the total FTH mRNA.

Human fetal brain has been shown to contain non ferritin mRNA (1.55kb) which hybridizes to the cDNA of 279nt of the FTH mRNA (4). To determine if the human adult brain contains a similar nonferritin mRNA, northern blot analysis was performed using polyA$^+$ RNA from the same. Also reported here are the results of this study.

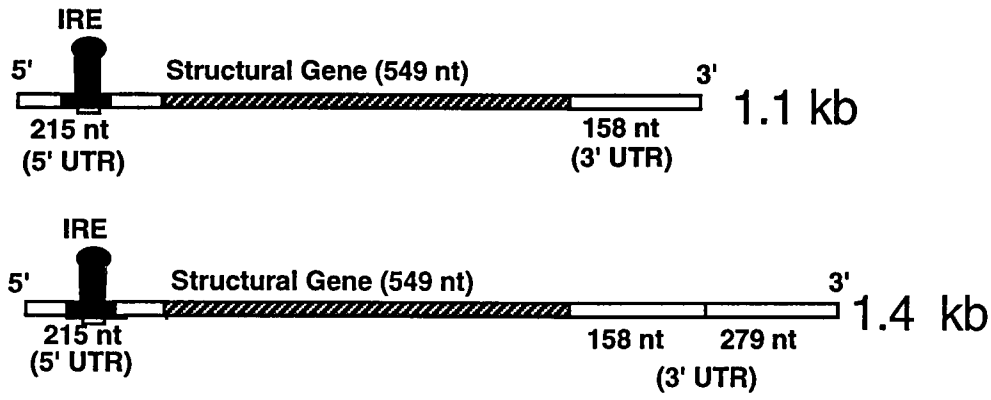

Fig. 2.1: Diagrammatic representation of the ferritin heavy chain mRNA's

Both mRNA's are identical in 5'UTR, coding region and 158nt of the 3'UTR. The 1.4kb mRNA has an additional 279nt in its 3'UTR. The stem-loop structure of the IRE in the 5'UTR is shown in solid black. Hatched portion of the mRNA's represents the coding region for 183 amino acids of the ferritin heavy chain.

Materials and methods

Samples and materials: Samples of normal adult brain were obtained from Duke University medical center, Durham, NC. Total RNA purified from these was used for reverse transcriptase polymerase chain reaction (RT-PCR). Specific oligonucleotides used as primers in RT-PCR were supplied by Oligos. Etc., Inc. (Guilford, CT). Human adult brain polyA$^+$ RNA used for northern blotting was supplied by Clontech (Palo Alto, CA). Electrophoresis reagents for southern and northern blots were supplied by United States Biochemical (Cleveland, OH). The enzymes: Taq polymerase, MMul-V reverse transcriptase, restriction enzymes EcoR1, Kpn1 and related buffers were supplied by Promega Corporation, Madison, WI. All other chemicals were of analytical grade, supplied by Sigma Chemical Company (St. Louis, MO).

Glassware and solutions: Glassware baked for 18 hours was used in northern and southern blotting. Distilled water treated with 0.1% diethyl pyrocarbonate for 24 hours and subsequently sterilized by autoclaving was used for preparing solutions for northern blotting.

RT-PCR: Total RNA from brain samples was isolated by guanidine-HCl method according to Sambrook et al (5). Specific

DNA primers were used for first strand synthesis and PCR. Fig. 2.2 shows the regions of mRNA to which the primers anneal. First strand synthesis was done using 15µg of total RNA pooled from the RNA preparations in a total volume of 50µl in two tubes using either primer A or B as described by Sambrook et al (6). A 5µl aliquot of the first strand from each tube was used for DNA amplification in corresponding tubes using primers A and C by the method of Maniatis (7). The thermal steps of PCR were: denaturation at 95 °C for 5 min, annealing at 60 °C for 1 min, polymerization at 72 °C for 2 min for 'n' number of cycles followed by 72 °C for 10 min for completion of polymerization. Fig 2.3 gives the amplification flow chart: tube 1 of PCR reaction represented the amplification of only the 1.4kb FTH mRNA while tube 2 represented the amplification of the total FTH mRNA. PCR was done varying the cycle number from 14 to 35 cycles.

Southern blotting and densitometry: The amplified DNA after each PCR was subjected to electrophoresis on a 1.2% agarose gel (Fig. 2.4), blotted and probed using the cDNA of FTH structural gene by the method of Maniatis et al (8). The blots were washed under high stringency (0.1% SSC, 0.1%SDS for 15min at room temperature and 65°C) and an autoradiographic image was obtained (Fig. 2.5). Densitometric scanning of autoradiograms was done using an LKB Bromma Ultrascan XL laser densitometer. The

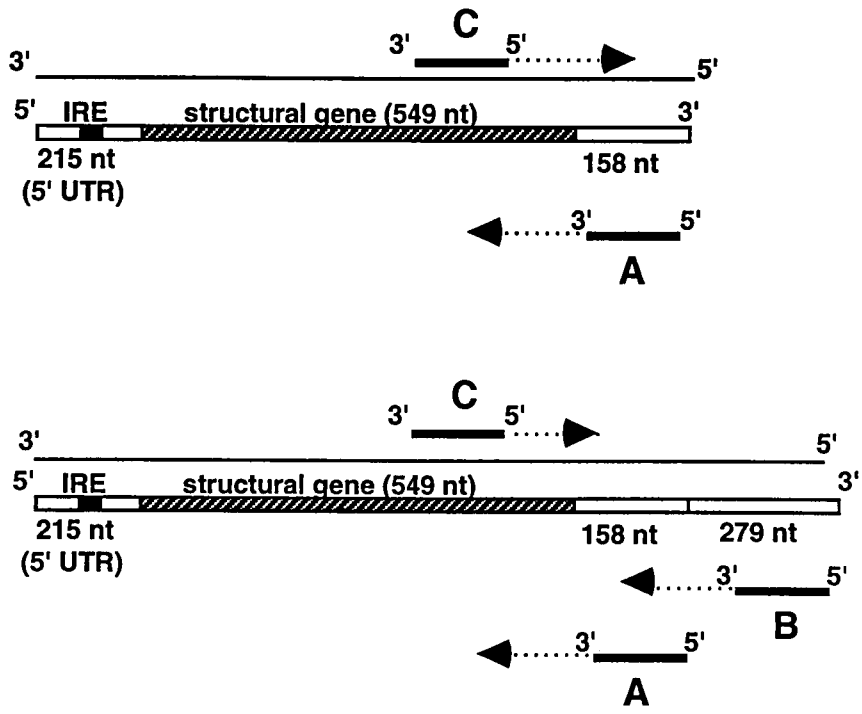

Fig. 2.2: Specific Primers used in RT-PCR
Primer A and B are complementary to the 3'UTR upstream to 279nt and to the 279nt regions respectively. Primer C is complementary to the coding region 302bp downstream to the translational start point. Primers A and B utilize both mRNA and cDNA as templates. Primer C utilizes only DNA as template. Solid lines represent DNA. Dotted lines and arrows represent the direction in which DNA is amplified by each specific primer.

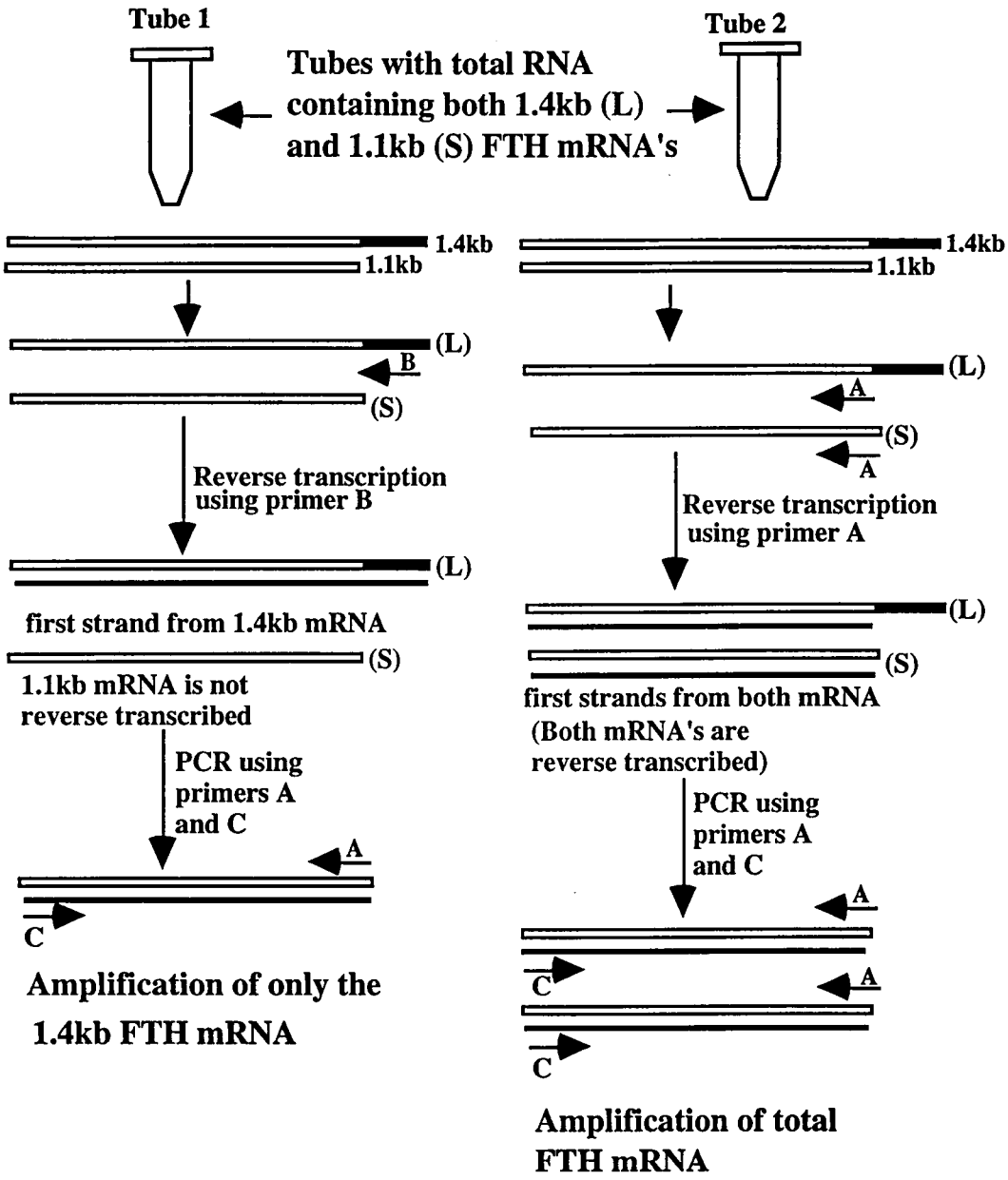

Fig. 2.3 Amplification flow chart of RT-PCR
Tube 1 represents the amplification of only the 1.4 kb FTH mRNA. Tube 2 represents the amplification of the total FTH mRNA. (L) represents the longer (or 1.4kb) mRNA while (S) represents the smaller (or 1.1kb) mRNA.

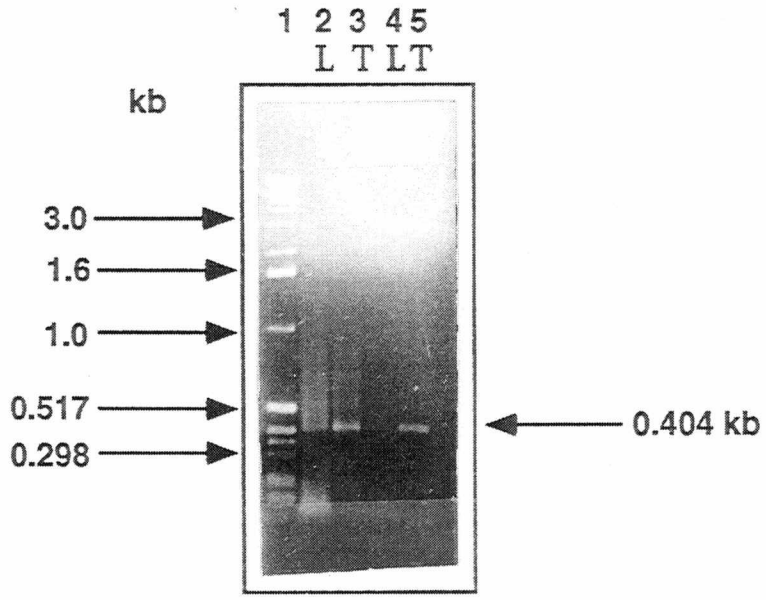

Fig. 2.4: RT-PCR amplification of the FTH transcripts in the human adult brain

Electrophoresis of the amplified DNA was carried out alongside molecular standards (lane 1: 1kb DNA ladder) on a 1.2% agarose gel. Lanes 2 and 3 were loaded with amplified DNA of 25 cycles of PCR while lanes 4 and 5 were loaded with amplified DNA of 33 cycles of PCR. L and T represent longer and total transcript respectively.

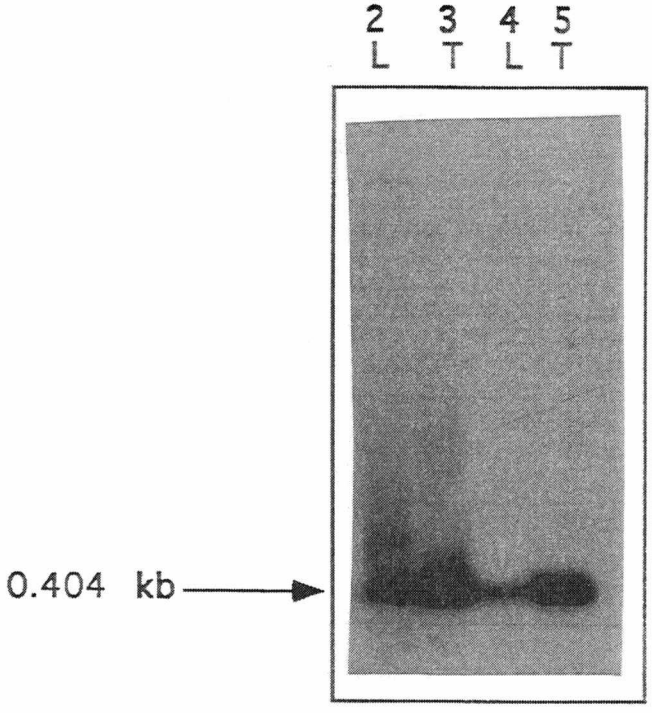

Fig. 2.5: Southern blot of RT-PCR amplification
Agarose gel in fig. 2.4 was blotted overnight for DNA transfer on to a nylon membrane that was then probed with radioactive cDNA of FTH structural gene (10^6 cpm). Subsequent high stringency washes were done with 0.1% SSC, 0.1% SDS at room temperature and 65°C for 15minuteseach. Lanes 2, 3, 4 and 5 correspond to the same lane numbers in the agarose gel in fig. 2.4.

darkness of the scanned bands was expressed in arbitrary units (AU).

Northern blot analysis: 1μg of polyA$^+$ RNA was used for northern blot analysis as described earlier (8). Using polyA$^+$ RNA in two different lanes of the same gel followed by blotting, two identical northern blots were obtained. Of the two blots, one was probed with cDNA of FTH structural gene and the other with cDNA of 279nt of the 3' UTR of the 1.4kb FTH mRNA. Subsequently, they were washed under high stringency conditions (twice with 0.2X SSC, 0.05% SDS for 15min at 50 °C) and autoradiographic images were obtained (Fig. 2.6). They were scanned densitometrically using BIORAD Model GS-670 imaging densitometer for band profiles (Fig. 2.7).

Results

Percentage contribution of 1.4kb FTH to total mRNA: Table 2.1 is a summary of results of RT-PCR. At PCR cycle numbers 14 and 15, no hybridization signal was seen indicating that the DNA was amplified in negligible amounts. Between the cycle numbers of 25 and 33, the percent contribution of the 1.4kb mRNA was calculated to be 25 - 30% of the total FTH mRNA. Beyond the cycle no. of 33, the percentage contribution was found to be 64.7%

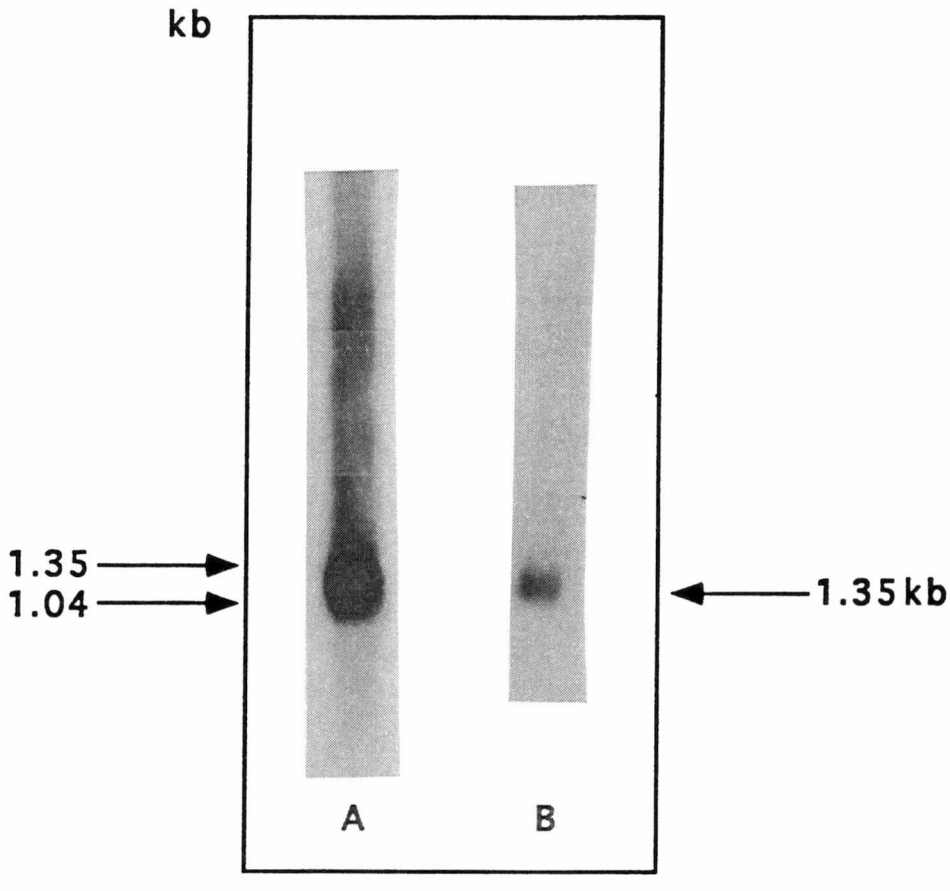

Fig. 2.6: Northern blot analysis of human adult brain polyA$^+$ RNA

Panel A shows a northern blot challenged with FTH structural gene. Bands 1.35 and 1.04kb correspond to the FTH mRNA's. Panel B shows an identical northern blot challenged with the cDNA of 279nt of the 3'UTR of the 1.4 kb FTH mRNA. The 1.35kb of the northern blot in panel B overlaps with the band due to the 1.4kb FTH mRNA of the northern blot in panel A.

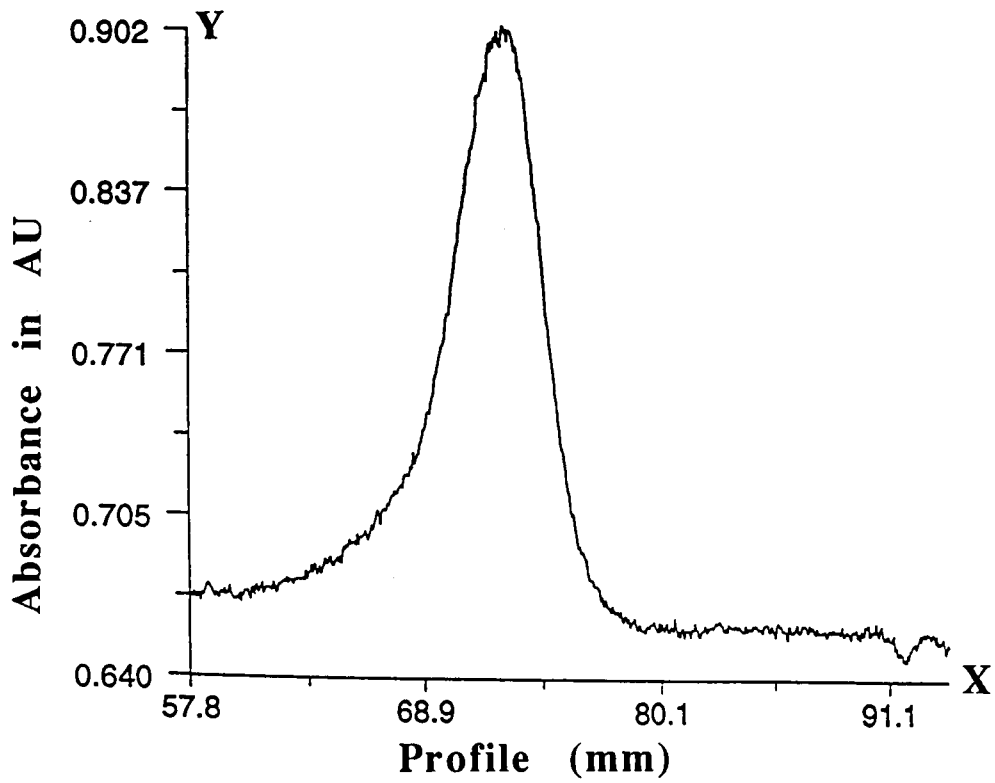

Fig 2.7: Peak profile of the autoradiogram of the northern blot of human adult brain polyA+ RNA The northern blot was probed with the cDNA of 279nt of the 3'UTR of the 1.4kb FTH mRNA. As seen above, a single peak indicates that a single hybridizing band is present in the human adult brain. This corresponds to the 1.4kb FTH mRNA.

Table 2.1: Results of densitometric scanning of autoradiograms of southern blots (RT-PCR)

Cycle no.	Contribution of larger transcript to total
14	Not detectable
15	Not detectable
25	24.5 %
28	30.15 %
30	31.16 %
33	31.7 %
35	64.7 %

Linear range of amplification of FTH mRNA lies between 14 and 33 cycles. At cycle numbers 14 and 15, negligible amounts of DNA result from amplification. So, no hybridization signal is observed. Between 25 and 33 cycles, percent contribution of longer to total transcript is 25 - 30%.

(Table 2.1). The linear range of PCR assay for the FTH mRNA therefore appears to be between 14 and 33 cycles.

Scanning of northern blots: Probing of the first northern blot with FTH structural gene showed a large band spanning 1.35 and 1.04kb (Fig. 2.6). Scanning of the second northern blot probed with cDNA of 279nt showed a single band of 1.35kb. This band overlapped with and was lighter than the band of similar molecular weight obtained on the first northern blot.

Discussion

The greater abundance of the 1.1kb FTH mRNA in the human liver has been shown earlier (3). Using the technique of RT-PCR, it has been demonstrated by this study that the 1.4kb FTH mRNA is about 2.33 times less abundant than the 1.1kb FTH mRNA in the human brain.

The significance of the novel sequence of 279nt in the 3' UTR of the 1.4kb FTH mRNA is yet to be understood. The presence of 279nt containing non-ferritin mRNA in the fetal brain and its absence in the adult brain is noteworthy. Changes in the genome during the life span of humans, as with any organism, are unlikely. The above observation, therefore, suggests the

occurrence of a development-dependent change in the human brain cells that results in the transcriptional switching off of a certain gene between the fetus and adult stages of life. This gene and its corresponding mRNA (1.55kb) remain to be identified. Differences in patterns of transcriptional regulation during development have been cited earlier. In 6-week old human embryos, the γ- globin gene is repressed (by methylation of DNA at the 5' position of the cytosine residues) whereas the ε- globin gene is actively transcribed. In 12 week old embryos, the γ- globin gene is derepressed (by demethylation) while the ε- globin gene is repressed (by *de-novo* methylation) (9). Similar examples of transcriptional regulation have been reported in *Xenopus* early embryos, in which, the TFIIIA factor is present in high concentration (ten copies per 5S gene) activating both somatic and oocyte type 5S rRNA genes. As development proceeds, the concentration of TFIIIA falls gradually. By gastrulation, the concentration of TFIIIA is about one copy per 5S gene and only the somatic type 5S gene is transcribed (10).

Band shift experiments using cytoplasmic extracts and 279nt region of the 1.4kb FTH mRNA could shed light on mRNA-protein interactions if they exist. *In-vitro* translation experiments with mRNAs containing both IRE and 279nt or either of them could reveal the role of 279nt in FTH synthesis.

References

1. Aisen, P. and Listowski, I. (1980) Ann. Rev. Biochem., 49, 357 -393.
2. Leibold, E.A. and Munro, H.N. (1988) Proc. Natl. Acad. Sci. USA., Vol 85, 2171 - 2175.
3. Dhar, M. S. and Joshi, J.G., (1993) J. Neurochemistry, 61, 2140 -2146.
4. Dhar, M., Chauthaiwale, V. and Joshi, J.G., (1993) Gene, 126, 275 - 278.
5. Sambrook, J., Fritsch, C.F. and Maniatis, T., (1989) in "Molecular Cloning: A laboratory manual", Cold Spring Harbor Laboratory Press, Second Edition, Vol I, 7.20 - 7.50.
6. Sambrook, J., Fritsch, C.F. and Maniatis, T., (1989) in "Molecular Cloning: A laboratory manual", Cold Spring Harbor Laboratory Press, Second Edition, Vol II, 8.11 - 8.13.
7. Sambrook, J., Fritsch, C.F. and Maniatis, T., (1989) in "Molecular Cloning: A laboratory manual", Cold Spring Harbor Laboratory Press, Second Edition, Vol II, 14.14 - 14.18.
8. Sambrook, J., Fritsch, C.F. and Maniatis, T., (1989) in "Molecular Cloning: A laboratory manual", Cold Spring Harbor Laboratory Press, Second Edition, Vol II, 9.31 - 9.55.
9. Mavilio, F., Giampaolo, A., Care, A., Migliaccio, G., Calandrini, M., Russo, G., Pagliardi, C.L., Mastroberardino, G., Marinucci, M., and

Peschle, C., (1983) PNAS, 80, 6907 - 6911.

10. Wolffe, A.P., and Brown, D.D., (1988) Science, 241, 1626 - 1632.

PART III

EFFECT OF ALUMINUM ON THE REGULATORY ENZYMES: ACONITASE AND ISOCITRATE DEHYDROGENASE

Summary

Aconitase and isocitrate dehydrogenase (ICDH) are the enzymes of the tricarboxylic acid (TCA) cycle. ICDH is an important regulatory enzyme of the TCA cycle while the enzyme cytoplasmic aconitase is a regulatory protein of ferritin synthesis. We show here that aconitase is not affected by aluminum whereas ICDH is inhibited by the metal ion in a concentration-dependent manner. Aluminum exhibits competitive inhibition of ICDH with respect to $NADP^+$ (K_i = 7.4 x 10^{-4} M).

Background

Aluminum (Al^{3+}) has been shown to inhibit several regulatory enzymes. Hexokinase and glucose-6-phosphate dehydrogenase, which catalyze the rate limiting steps of glycolysis and the pentose phosphate pathway respectively are both inhibited by Al^{3+} (1,2). Similarly, Al^{3+} inhibits high affinity choline transport which is the rate limiting step in acetylcholine synthesis and reflects the cholinergic activity, vital to memory and learning *in-vivo* (3). The GTPase activity of rod photoreceptor G-protein, G_V is inhibited in the presence of 4 x 10^{-10}M free Al^{3+} ion as the magnesium ion concentration is reduced from 1 x10^{-3} to 5 x 10^{-5}M (4). There is also evidence that Al^{3+} binds to the iron storage protein, ferritin and decreases the rate of iron uptake by the protein (5). The resultant unsequestered iron may lead to increased ferritin synthesis.

The aim of this study was to investigate the effect of Al^{3+} on two regulatory enzymes, namely aconitase and isocitric dehydrogenase (ICDH).

Materials and Methods

Materials: The enzymes aconitase and ICDH, were isolated from porcine heart and supplied in a highly purified form by Sigma Chemical Company (St. Louis, MO). All other chemicals were of analytical grade and supplied by Fisher Scientific Company (Fair Lawn, NJ) and Sigma Chemical Company (St.Louis, MO).

Aconitase activity: Aconitase activity was measured using the coupled method of Rose and Connell (6). The enzyme was activated before use by preincubation with ferrousammoniumsulfate ($Fe(NH_4)_2(SO_4)_2$) (5 x 10^{-3} M) and cysteine (1 x 10^{-2} M, pH adjusted to 7.4) in a buffer of Tris.HCl (0.1M, pH 7.4) for 30 minutes at 4°C. The enzyme activity was then assayed at 25°C by addition of aconitase to a 1ml reaction mix which was an aqueous solution containing a final concentration of 0.1M Tris.Cl (pH 7.0), 1 x 10^{-3}M magnesium chloride, 1 x 10^{-3}M $NADP^+$, 1 x 10^{-3}M sodiumcitrate and 1U of ICDH. The absorbance of reduced $NADP^+$ at 340nm was measured using a Beckman uv-visible spectrophotometer.

Isocitrate dehydrogenase activity: ICDH was assayed using the method of Ochoa (7) also by measuring the absorbance of reduced $NADP^+$ at 340nm using a Beckman uv-visible

spectrophotometer. This assay involves addition of 0.06U of ICDH to a reaction mix. The reaction mix was a 1ml aqueous solution containing final concentrations of 2.5 x 10^{-2}M HEPES (pH 7.4), 6.0 x 10^{-4}M manganese chloride, 4.5 x 10^{-5}M $NADP^+$ and 2 x 10^{-4}M dl-isocitrate.

Inhibition by Al: An aqueous stock of 0.01M aluminum chloride ($AlCl_3.6H_2O$) was freshly prepared. To obtain a final concentration of the metal ion in the assay, a calculated volume of the stock was added to the reaction mix and thoroughly mixed by inverting before the addition of enzyme.

Presentation of data: The readings of optical density(OD) were noted every minute for 5 minutes for aconitase activity and the average change in OD per minute was used as the control (100%) activity. For ICDH activity, the readings of OD were noted every 15 seconds for 75 seconds and the average change for 15 seconds was used as the control (100%) activity. The OD change observed in the presence of various concentrations of Al^{3+} was expressed as percent of the control activity for both enzymes. Concentration of free $NADP^+$ was calculated using the relation:

$$\delta Absorbance = K_e.\ [NADP^+\text{-}AlCl_3]$$

$$[NADP^+]_{total} = [NADP^+]_{free} + [NADP^+\text{-}AlCl_3]$$

δAbsorbance was taken as the negative absorbance value obtained at a $AlCl_3/[NADP^+]$ ratio of 1.0 from spectral studies.

Results

Effect of Al on aconitase activity: The enzyme aconitase was not inhibited by the presence of high Al^{3+} concentration (up to 6 x 10^{-4} M) during assay. Preincubation of the enzyme prior to, or after activation with $(Fe(NH_4)_2(SO_4)_2)$ showed no inhibition of enzyme activity.

Effect of Al on ICDH: ICDH was inhibited by $AlCl_3$ in a concentration dependent manner (Fig 3.1). The residual enzyme activity was dependent solely on the final concentration of the metal ion during assay. The enzyme was not inhibited by similar high concentration of sodium chloride suggesting that the observed inhibition was not due to chloride ions. Preincubation with $AlCl_3$ had no effect on enzyme activity. The inhibition was reversible by dilution and independent of time (Fig 3.2). At pH 6.0, 6.5, 7.3,7.5 and 8.0 the ICDH enzyme showed residual activity close to 57% (Fig 3.3). Validity of results beyond pH 8.0 is not clear because of very low solubility of Al^{3+} at alkaline pH. Spectra of the enzyme in the presence of Al^{3+} showed no evidence of metal ion binding to the ICDH enzyme.

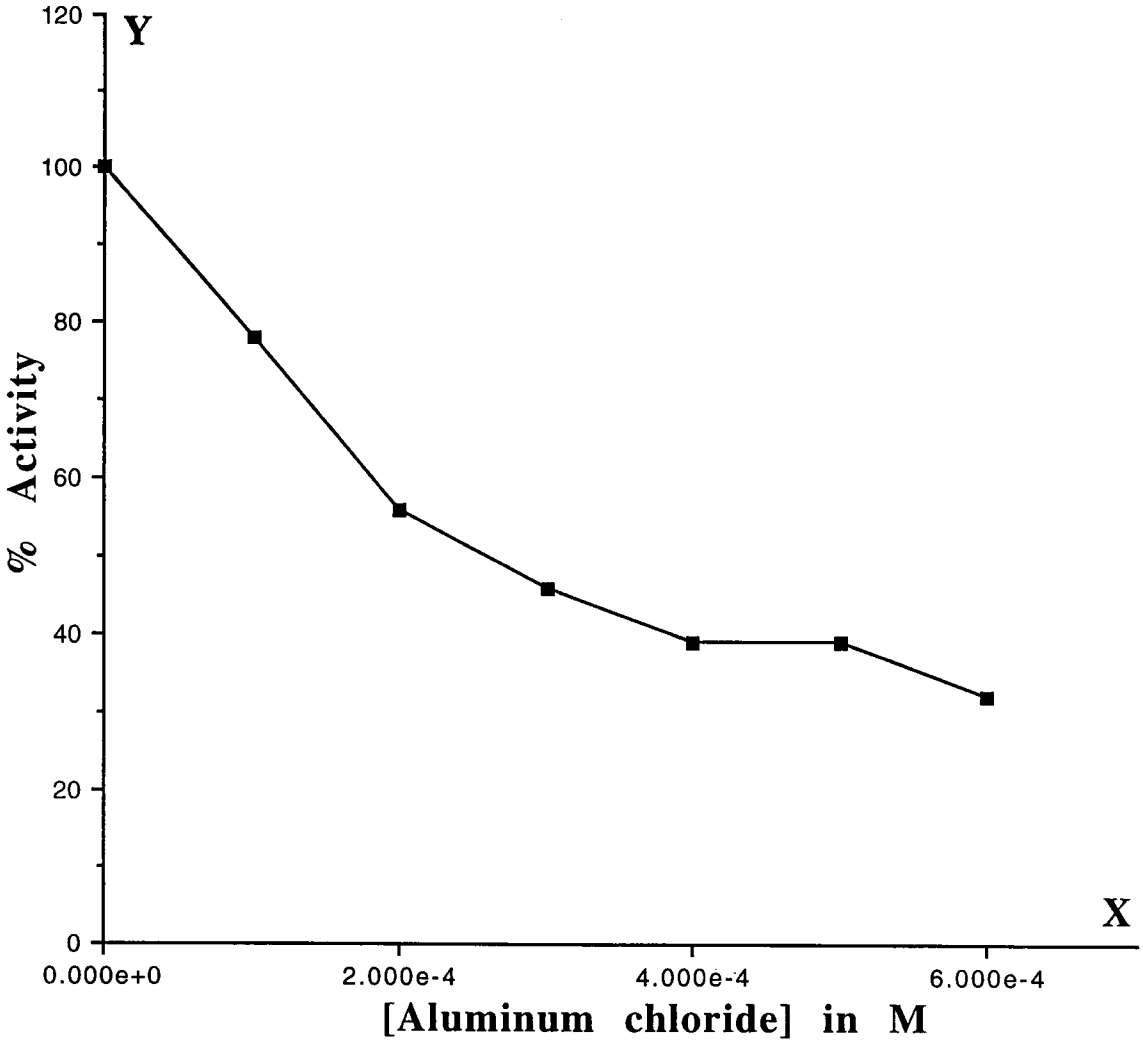

Fig. 3.1: Effect of Al^{3+} on ICDH activity

Increasing concentrations of $AlCl_3.6H_2O$ were added to the reaction mix that contained 2.5 x 10^{-2} M HEPES, 6.0 x 10^{-4} M $MnCl_2$, 4.5 x 10^{-4} M $NADP^+$, 2 x 10^{-4} M dl-isocitrate and 0.06 U of ICDH at pH 7.3 and at a temperature of 25° C.

Al^{3+} inhibited the enzyme in a concentration dependent manner. Residual activity at a final concentration of 6 x 10^{-4} M of $AlCl_3.6H_2O$ was 30%.

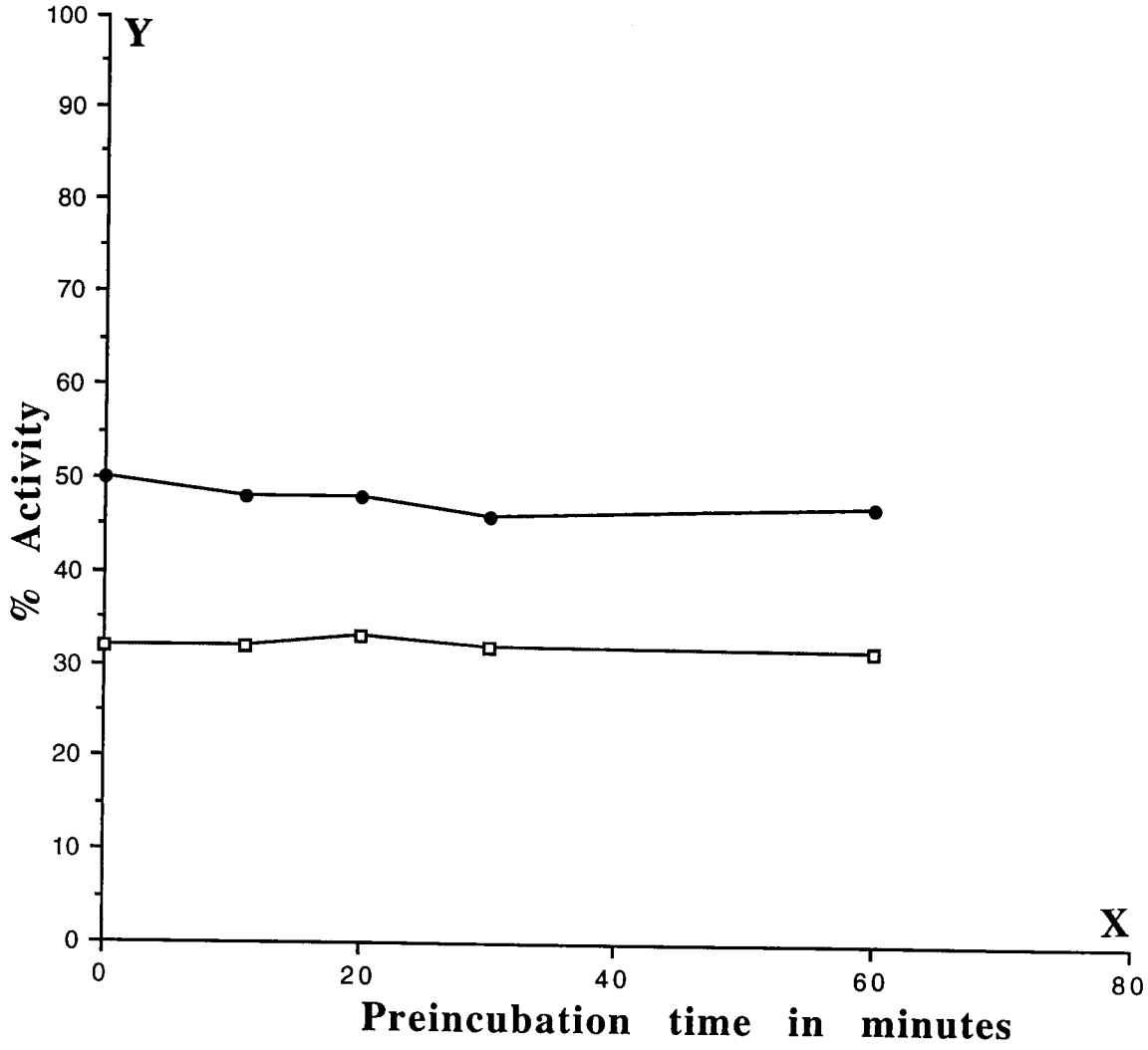

Fig. 3.2: Effect of presence of Al^{3+} during preincubation and assay

ICDH was preincubated with $AlCl_3.6H_2O$ for varying periods of time prior to assaying enzyme activity in the presence of the same Al^{3+} concentration. The enzyme activity observed depended only on the final concentration of $AlCl_3.6H_2O$ during the assay. Preincubation and assay at a final Al^{3+} concentration of 3.2×10^{-4} M (●) and 6.0×10^{-4}M (○) are shown in the above figure.

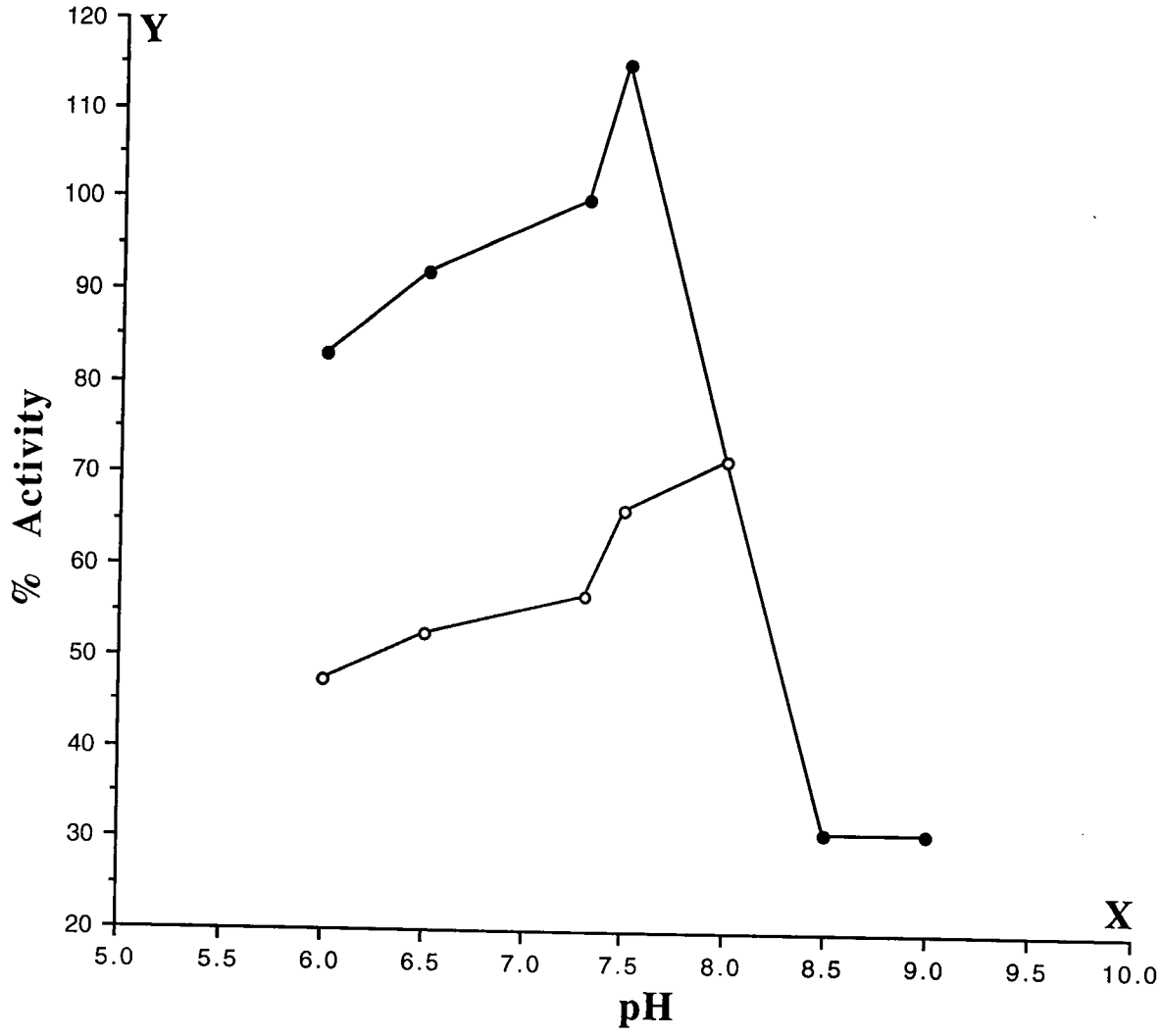

Fig. 3.3: Effect of Al^{3+} on the pH curve of ICDH
Inhibition of ICDH activity by Al^{3+} occured between pH's 6.0 and 7.5. The residual activity was approximately 56% of the control activity within the 6.0 - 7.5 pH range. Percent enzyme activity at different pH's is shown in the absence (●) and presence (○) of 2.5×10^{-4} M $AlCl_3$.

In the presence of $AlCl_3$, $NADP^+$ showed a negative absorbance spectrum with a negative absorbance peak at 260 nm. The negative absorbance increased with an increase in $Al^{3+}/NADP^+$ ratio from 0.2 to 1.0 (Fig 3.4 (a), (b) and Table 3.1). Beyond the ratio of 1.0, no significant increase in negative absorbance values was observed. The metal ion exhibited a competitive inhibition of the ICDH enzyme with respect to $NADP^+$ (Fig 3.5). The K_i of inhibition was calculated to be 7.4 $x10^{-4}$ M (Fig 3.6). A slope of 1.12 was obtained on the Johnson-Eyring plot (Fig 3.7). The metal ion showed no effect on the manganese utilization by the ICDH system.

Discussion

The enzyme cytoplasmic aconitase has been shown to be identical to the regulatory protein of ferritin synthesis namely, iron responsive element binding protein (IRE-BP) (8). Both proteins contain an Fe-S cluster and both bind RNA when the cluster is not fully filled. In the 4Fe-4S status of the cluster, both proteins are active as aconitase with a corresponding loss of RNA-binding activity. Comparision of the aconitase purified from cytoplasmic extracts shows that it is strikingly similar to the published sequence of IRE-BP in its amino acid composition, molecular weight, isoelectric point and the sequences of six random peptides.

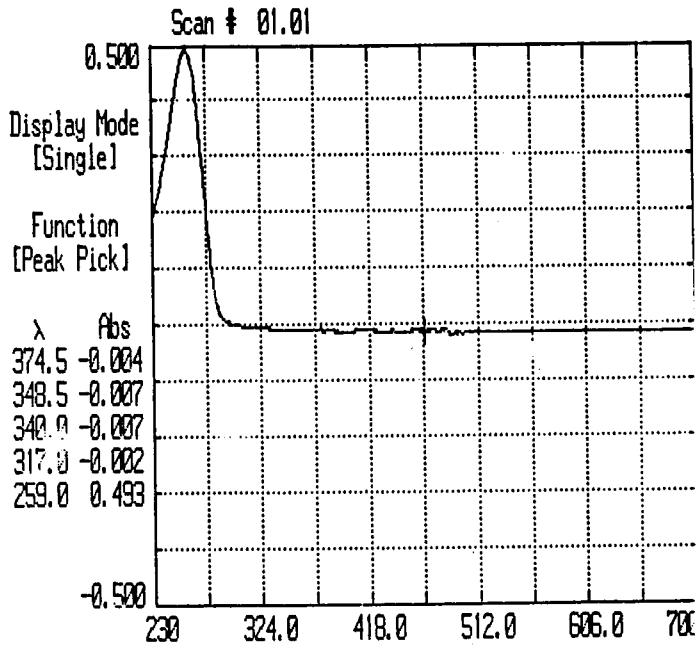

Fig. 3.4 (a): Normal absorbance spectrum of $NADP^+$

Final concentrations of $NADP^+$ and HEPES (pH 7.4) were 4.5×10^{-4}M and 2.5×10^{-2}M respectively. Absorbance peak of $NADP^+$ was seen at 260nm.

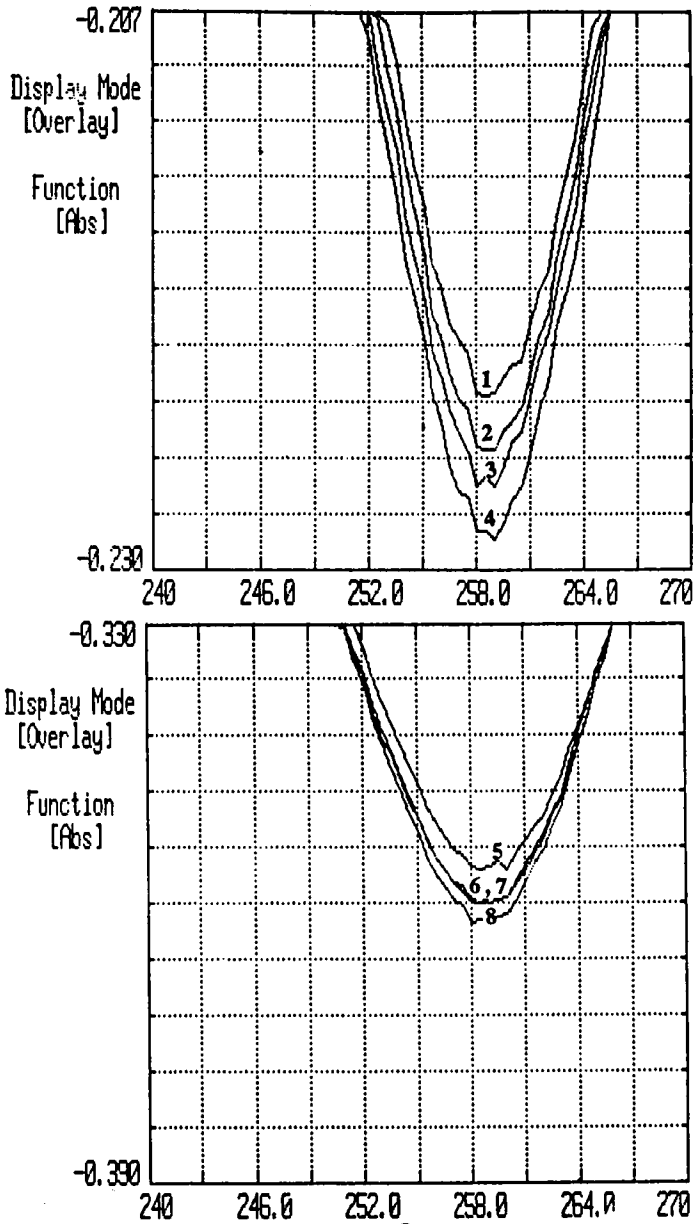

Fig. 3.4 (b): Effect of Al^{3+} on the spectrum of $NADP^+$

Final concentrations of $NADP^+$ and HEPES (pH 7.4) were 4.5×10^{-4}M and 2.5×10^{-2}M respectively. Difference spectra 1 - 8 were obtained by increasing the concentration of $AlCl_3.6H_2O$. Table 3.1 gives the $Al^{3+}/NADP^+$ ratios and corresponding values of negative absorbance.

Table 3.1: Negative absorbance of $NADP^+$ at 260nm

Scan no.	$AlCl_3/NADP^+$ ratio	Negative absorbance
1	0.2	-0.2215
2	0.3	-0.2238
3	0.4	-0.2247
4	0.8	-0.2271
5	1.6	-0.3561
6	3.2	-0.3591
7	4.0	-0.3591
8	5.0	-0.36

Final concentrations of $NADP^+$ and HEPES (pH 7.4) were $4.5 \times 10^{-5}M$ and $2.5 \times 10^{-2}M$ respectively.

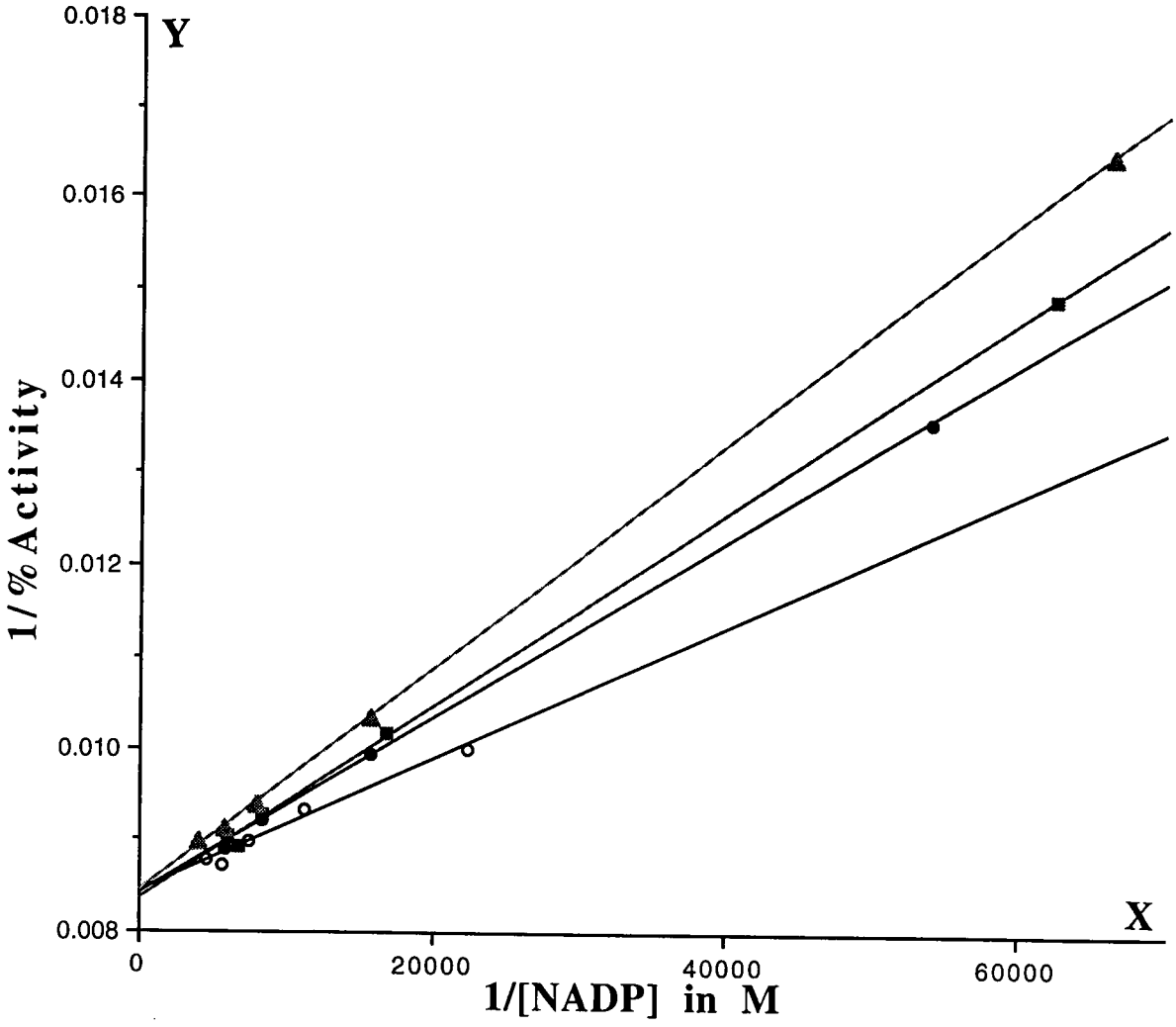

Fig. 3.5: Effect of Al^{3+} on $NADP^+$ utilization
The metal ion bound $NADP^+$ in a competitive manner, increaing the K_m of the enzyme for $NADP^+$. V_{max} was unaltered. The graph points of control (∘), final concentrations of $AlCl_3$ of 2.5 x 10^{-4} M (●), 3.2 x 10^{-4} M (■) and 5.0 x 10^{-4} M (▲) are shown in the above figure.

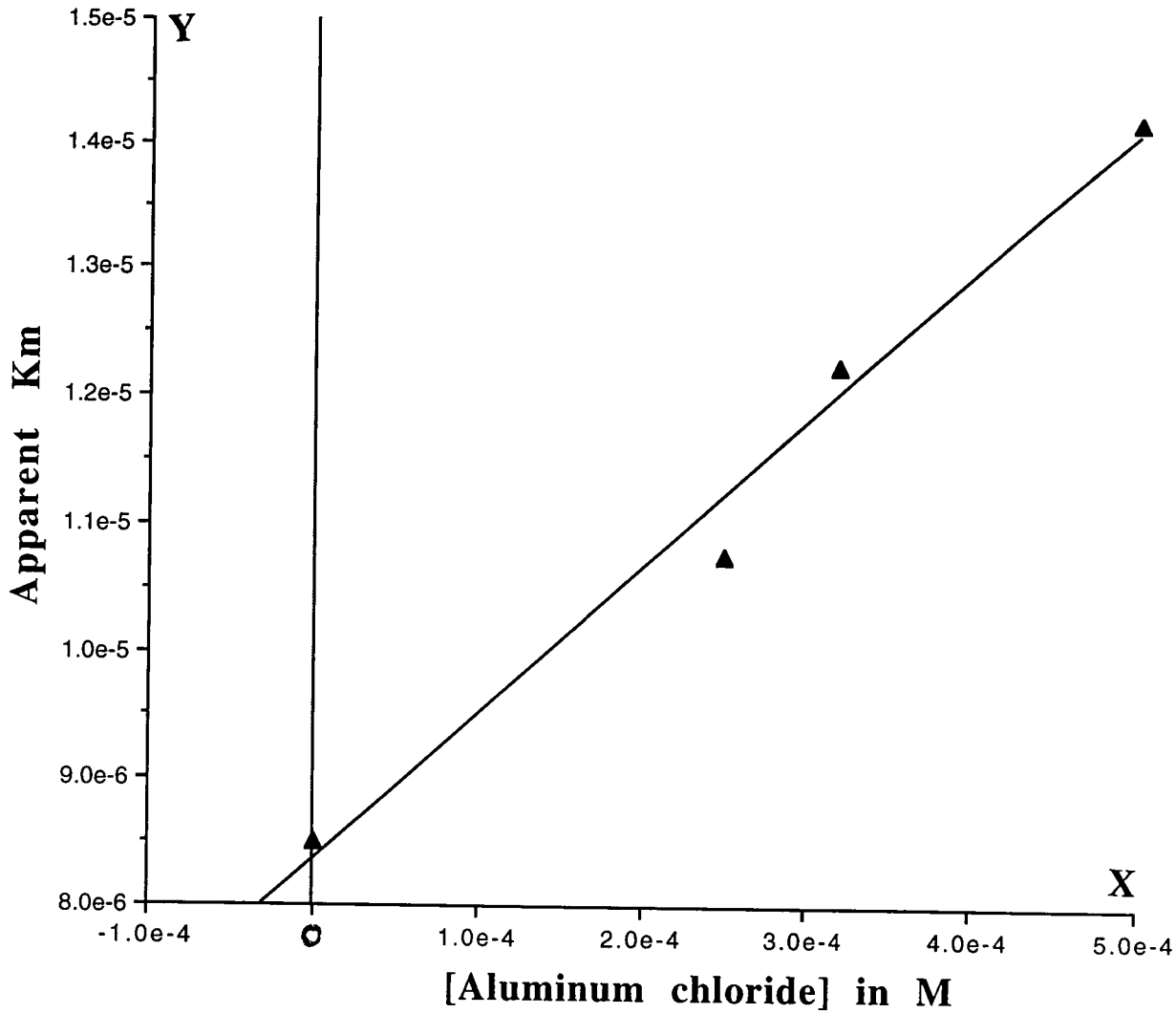

Fig. 3.6: K_i of inhibition by Al^{3+}
The apparent K_m (from Fig. 2.5) was plotted versus the corresponding $AlCl_3$ concentration. The x-intercept gave the K_i of inhibition (7.4×10^{-4} M).

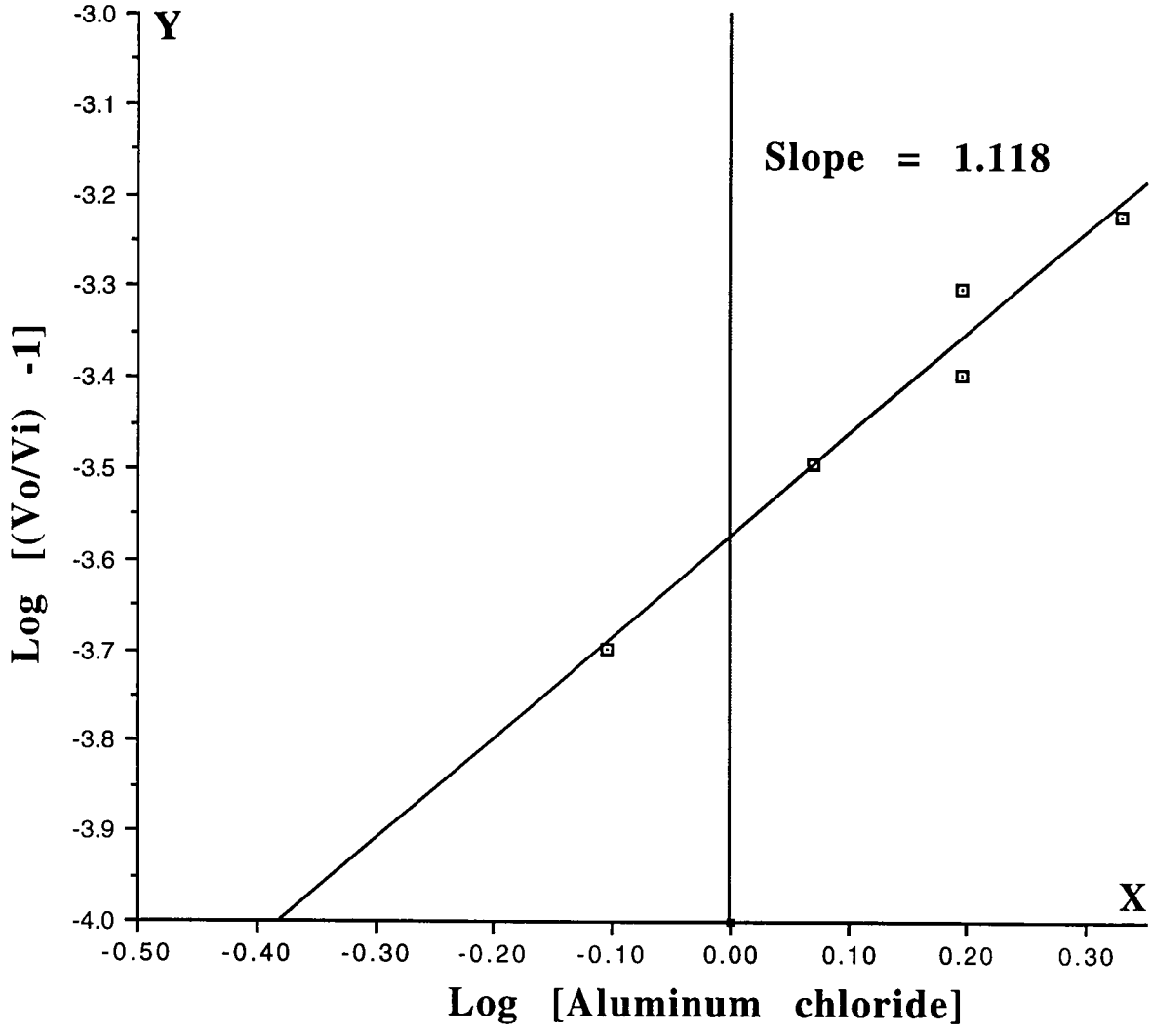

Fig. 3.7: Johnson-Eyring plot

The slope on the Johnson-Eyring plot gives the number of Al^{3+} ions combining with each molecule of $NADP^{+}$.
V_i and V_o are the velocities of the ICDH reaction with and without $AlCl_3$ respectively. The slope of the best fitting line was calculated to be 1.118 indicating that the binding of Al^{3+} to $NADP^{+}$ is 1:1.

Thus, by the loss or gain of Fe atoms in its Fe-S cluster, the same protein functions either as an RNA binding repressor(IRE-BP) or as an active enzyme (c-aconitase) (Fig 3.8). Experimental results show that the enzyme aconitase is not affected by Al^{3+}. As the protein is the same as the iron regulatory protein, IRE-BP, it is highly unlikely that the metal ion exercises any effect on ferritin synthesis via the repressor protein.

In living systems, the tricarboxylic acid cycle (TCA) is an important metabolic pathway in the complete utilization of glucose. The formation of citrate (from oxaloacetate and acetyl-CoA) and the formation of α- ketoglutarate (from isocitrate) are the two control points of the TCA cycle. The enzymes citrate synthase and ICDH are the corresponding allosteric regulatory enzymes. By dehydrogenation and decarboxylation, the ICDH converts isocitrate to α-ketoglutarate. By the removal of isocitrate, a product (and substrate) of the aconitase reaction, ICDH pulls the equilibrium of the aconitase reaction towards the utilization of citrate to form isocitrate. The enzyme aconitase has the highest affinity for isocitrate (4.8×10^{-4}M) among its three substrates, citrate, cis-aconitate and isocitrate). The relative velocity for the conversion of isocitrate to citrate is the highest among the reactions catalyzed by the aconitase enzyme (9).

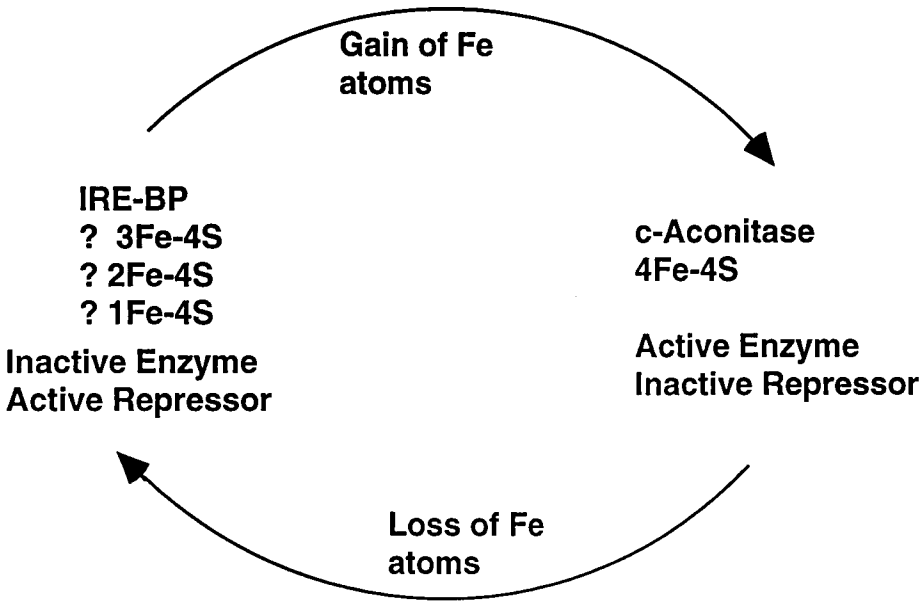

Fig. 3.8: The relation between the two roles of cytoplasmic aconitase

The same protein alternates between RNA binding repressor and active enzyme roles by the loss or gain of iron atoms in the iron-sulfur cluster. Both roles are mutually exclusive. The status of the active enzyme form is 4Fe-4S. Cluster status of the active repressor has not yet been identified.

It has been shown in this study that Al^{3+} inhibits ICDH by forming an Al-$NADP^+$ complex, thereby reducing the concentration of free $NADP^+$ and increasing the K_m of the enzyme for $NADP^+$ in vitro. The slope of 1.12 on the Johnson-Eyring plot indicates that the binding of the metal ion to $NADP^+$ is 1:1. This is corroborated by the spectra of $NADP^+$ in the presence of Al^{3+} which show an increase in negative absorbance with an increase in $Al^{3+}/NADP^+$ ratio. Beyond the ratio of 1.0, no significant increase in negative absorbance of $NADP^+$ is observed, further confirming the 1:1 binding of Al^{3+} to $NADP^+$.

A similar inhibition *in-vivo*, as observed by this study could result in accumulation of isocitrate in the cell. This, in turn, could cause the accumulation of citrate due to cellular aconitase activity. Inhibition of ICDH by Al^{3+} therefore could deregulate the TCA cycle at the first two control points as shown in Fig.3.9.

Numerous oxidation reactions *in-vivo* use $NADP^+$ as the hydrogen acceptor. Al ion may inhibit many of these by forming Al-$NADP^+$ complex due to electrostatic attractions between the cation and the negatively charged phosphate groups of $NADP^+$. Earlier studies have revealed that Al^{3+} inhibits several enzymes with ATP as a substrate. This occurs because ATP tends to form a stronger complex with Al^{3+} than with Mg^{2+} and Al^{3+}-ATP acts as a very

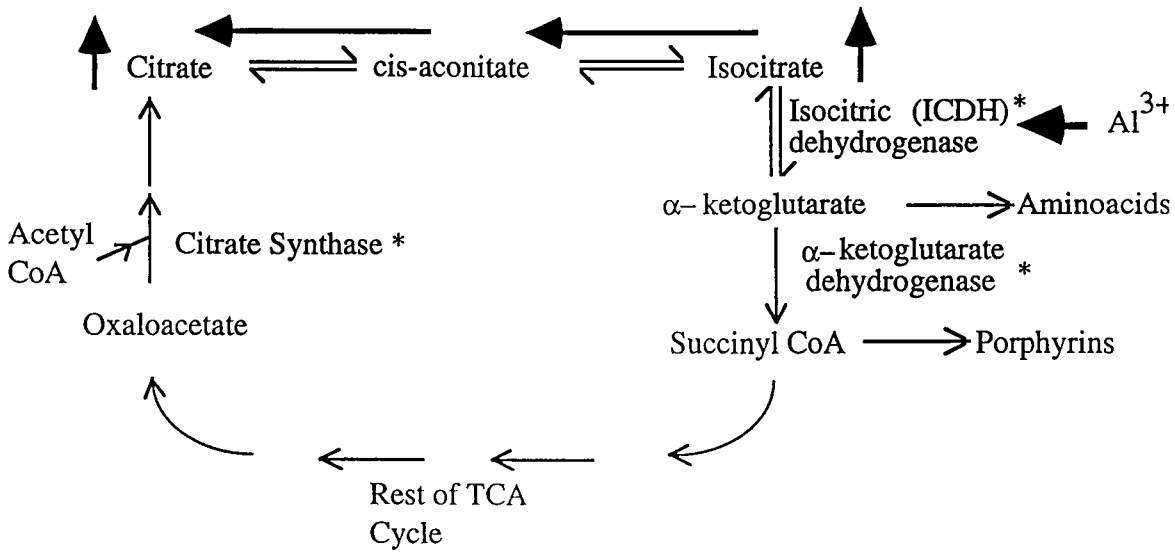

Fig. 3.9: Possible deregulation of the TCA cycle by Al^{3+}

The TCA cycle is regulated at three control points. (*) indicates regulatory enzymes. Al^{3+} inhibits ICDH causing accumulation of isocitrate. Due to the higher affinity of aconitase for isocitrate, this in turn could cause accumulation of citrate. Thin arrows show the normal functioning of the cycle. Bold arrows show inhibition by Al^{3+} and possible deregulation of the TCA cycle.

strong competitor for Mg^{2+}-ATP complex (10). Chromatin and DNA are cell structures that are most vulnerable to Al^{3+}. The metal ion probably binds to the phosphate groups on DNA with an Al^{3+}/DNA-P ratio of 1:3. However, excess Al^{3+} can increase the ratio to greater than 2:1, most likely due to binding of OH^- ions as well (11). All of the above evidence suggests that the metal ion may interfere with various pathways of cellular metabolism probably by binding negatively charged groups on biomolecules and inhibiting their normal function.

References

1. Womack, F. C. and Colowick, S. P., 1979, Proc. Natl. Acad. Sci., vol. 76 no. 10, 5080- 5084.
2. Cho, S. W. and Joshi, J. G., 1989, Biochemistry, 28, 3613 - 3618.
3. Johnson, G. V. W. and Jope, R. S., 1986, Toxicology, 40, 93 - 102.
4. Miller, J. L., Hubbard, C. M., Litman, B. J. and Macdonald, T. L., 1989, J. Biol. Chem., vol 264 no. 1, 243 - 250.
5. Fleming, J. T. and Joshi, J. G., 1991, Neurobiology of Aging, vol. 12, 413 - 418.
6. Rose, I. A. and O'Connell, E. L., 1967, J. Biol. Chem., 242 no. 8, 1870 - 1879.
7. Ochoa, S., 1948, J. Biol. Chem., 174, 133-137.
8. Kennedy, M. C., Mueller, L. M., Blondin, G. A. and Beinert, H., 1992, Proc. Natl. Acad. Sci., vol 89, 11730 - 11734.
9. Barman, T. E., 1985, "Enzyme Handbook", vol II, Springer Verlag, New York.
10. Ganrot, P. O., 1986, Environmental Health Perspectives, vol 65, 363 - 441.
11. Matsumoto, H. E., Hirasawa, E., Torikai, H. and Takahashi, E., 1976, Plant Cell Physiol., 17, 127 - 137.

IMPLICATIONS FOR FURTHER WORK

This study has revealed that the 1.1kb FTH mRNA is in greater abundance over the 1.4kb mRNA in the human brain. To date, no explanation is at hand for the role of the 279nt in the 3'UTR of the FTH mRNA. Its presence in the 1.4kb FTH mRNA and in a nonferritin mRNA (yet not identified) in the human fetal brain suggests that it may be of significance in translational regulation and in development. A second IRE binding protein, IRF_b, different from the earlier characterized IRE-BP is noteworthy. Gel shift assays using the 1.4kb FTH mRNA and cytoplasmic extracts from mammalian cells may reveal if proteins that bind the 279 nt are present in the cytoplasm. If such proteins are present, experiments must be done to investigate if they interact with the IRE-IREBP and IRE-IRF_b complexes.

In-vitro translation experiments using the FTH mRNA's with or without the 279nt (of the 3'UTR) and the IRE (of the 5'UTR) may reveal the role of 279nt in FTH synthesis in the presence and absence of IRE. Half-life and mRNA decay studies of the 1.4 kb FTH mRNA could reveal the role of the 279nt in its stability.

This study also dealt with the inhibition by Al^{3+} of the isocitrate dehydrogenase enzyme isolated from porcine heart. Inhibition

studies with Al^{3+} could be done using the enzymes isolated from the human heart and brain.

VITA

Sudha Sunil Chhaya was born in Rajahmundry, A.P., India on December 22, 1969. She attended school in Madras, T.N. and graduated from Padma Seshadri Bala Bhavan Junior College in May 1986. She entered the University of Madras in June, 1986 and graduated with a Bachelor of Science degree in Botany with the ancillary subjects, Chemistry and Zoology in May 1989. In 1989, she was awarded the University First Rank and the University Gold Medal for her undergraduate study.

In August 1989, she was awarded the Government of India Scholarship at the University of Madras. She graduated with a Master's degree in Biochemistry in May 1991.

In the Fall of 1992, she accepted a graduate teaching assistantship at the University of Tennessee, Knoxville and began her graduate study in Biochemistry. She received a second Master's degree in Biochemistry in June 1995